dition to [^{3}H]E_1S, the transport of other organic anions was examined in ABCG2-expressing membrane vesicles. As shown in Fig. 5, [^{3}H]DHEAS, a steroidal sulfate conjugate, was accepted by ABCG2 as a substrate. Furthermore, the uptake of E3040S and E3040G was examined at 2.5 μM, and it was found that the uptake of E3040S (900 pmol/mg/5 min) was much higher than that of E3040G (12.5 pmol/mg/5 min) (Fig. 5). Sulfate-preferential transport was also observed for 4-MU, although we cannot directly compare the absolute values of the uptake between 4-MUS and 4-MUG, because the medium concentrations for 4-MUS and 4-MUG were 5.0 and 4.1 μM, respectively (Fig. 5). [^{3}H]Methotrexate, [^{3}H]$E_2$17βG, and [^{3}H]DNP-SG were also transported by ABCG2 to a much lesser extent than with sulfate conjugates (Fig. 5). ABCG2-mediated transport levels of [^{3}H]taurocholic acid or [^{3}H]TLC-S were not significant under the experimental conditions used (Fig. 5).

Kinetic analysis was also performed for ABCG2-mediated transport of [^{35}S]4-MUS and [^{35}S]E3040S. As shown in Fig. 6, the K_m values for [^{35}S]4-MUS and [^{35}S]E3040 were 12.9 ± 2.1 μM and 26.9 ± 4.0 μM, respectively.

DISCUSSION

We examined the function of ABCG2 by using membrane vesicles prepared from the wild type human *ABCG2*-transfected mouse lymphoma cells (P388 cells) and suggested that the sulfated conjugates of steroids and xenobiotics are preferentially transported by this transporter. However, the use of mouse lymphoma cells has disadvantages, because the presence of an unknown amount of related mouse proteins may significantly influence the results.

In the present study, it was suggested that E_1S and DHEAS are the potential endogenous substrates for ABCG2 (Figs. 1 and 5), although *in vivo* experiments are required to clarify its physiological significance. In addition, sulfate conjugates of xenobiotics are also preferentially transported by ABCG2 (Fig. 5). However, the affinity for ABCG2-mediated E_1S transport (K_m = 16.6 μM, Fig. 3) was lower than that for MRP1-mediated transport; the K_m values for E_1S were 4.2 and 0.73 μM in the absence and presence of GSH (19).

If we consider the fact that MRP1, another transporter capable of transporting sulfated conjugates, is highly expressed on testicular Leydig cells, which is the major site of sulfate conjugation of estrogen in the testis, it is possible that MRP1 protects the testis from exposure to cytotoxic compounds by extruding them after conversion into sulfate conjugates (19). ABCG2 may also play a host defensive role by being expressed in placenta, liver, and intestine, where sulfotransferase activity is very high with minimal MRP1 expression (6, 14, 29). Moreover, the apical localization of ABCG2 is in marked contrast to the basolateral localization of MRP1 (6, 11). Collectively, it is possible that the apically located ABCG2 in placenta, liver, and intestine may be responsible for protection of the fetus, biliary excretion, and prevention of xenobiotic absorption, respectively, whereas basolaterally localized MRP1 in testis is responsible for protecting the germ line (19).

The inhibitory effect of several compounds on the ABCG2-mediated transport of E_1S needs to be discussed in relation to their chemical structure. No potent inhibitory effect was observed up to 80 and 2 μM for DNP-SG and LTC_4, respectively, on ABCG2-mediated E_1S transport (Table II). In addition, $E_2$17βG and E3040G did not potently inhibit ABCG2 function up to 75 and 250 μM, respectively (Table II). In contrast to the much lower sensitivity toward glutathione and glucuronide conjugates, many sulfated conjugates reduced ABCG2-mediated transport (Fig. 4 and Table I). The approximate IC_{50} values of DHEAS, PNPS, 4-MUS, and E3040S were 55, 53, 6, and 10 μM, respectively (Fig. 4 and Table I). Collectively, it appears that ABCG2 preferentially recognizes sulfated conjugates.

In addition to E_1S, DHEAS was also transported by ABCG2 (Fig. 5). It is noteworthy that 4-MUS and E3040S, but not 4-MUG or E3040G, were extensively transported by ABCG2 (Fig. 5 and 6), and the IC_{50} values of 4-MUS and E3040S for the ABCG2-mediated transport of E_1S were 6 and 10 μM, respectively (Fig. 4 and Table I), whereas 4-MUG or E3040G did not potently inhibit this transport up to 500 and 250 μM, respectively (Table II). Although TLC-S inhibited the ABCG2-mediated transport with an IC_{50} of less than 50 μM (Fig. 4 and Table I), TLC-S was not significantly transported by ABCG2 under the present experimental conditions (Fig. 5). These results may be accounted for by assuming that ABCG2 has minimal V_{max} value for TLC-S. We also found ABCG2-mediated transport of MRP substrates, such as methotrexate and $E_2$17βG, although these compounds are transported to a much lesser extent compared with E_1S (Figs. 1 and 5). Indeed, their affinity for ABCG2 was quite low, because 600 μM methotrexate or 75 μM $E_2$17βG did not significantly inhibit the ABCG2-mediated transport of E_1S (Table II).

The affinity of anti-tumor drugs for ABCG2 should be discussed in relation to resistance to this anti-tumor drug because of the previous finding that ABCG2-expressing cells acquired resistance against these drugs (1, 30, 31). Concerning the resistance of ABCG2-overexpressing cells against SN-38, it has been demonstrated that ABCG2 transports this drug with a K_m value of 4.0 μM (32). The finding that that IC_{50} value of SN-38 on ABCG2-mediated transport of E_1S is ~1.6 μM (Fig. 4 and Table I) is consistent with this previously reported K_m value (32). It was also suggested that daunomycin, mitoxantrone, and doxorubicin have low affinity for ABCG2 (Fig. 4 and Table I). Such transport characteristics mediated by ABCG2 should also be discussed in relation to the mutation in its gene structure. It has been reported that the amino acid at 482 plays an important role in determining the substrate specificity of ABCG2 (33). For example, ABCG2 containing a Thr or Gly residue at position 482 transports rhodamine 123 and the anthracyclines (doxorubicin and daunorubicin), whereas wild type ABCG2 containing an Arg at this position does not (33). In contrast, all three ABCG2 variants transport mitoxantrone (33). Moreover, the overexpression of ABCG2 containing an Arg residue at position 482, but not those containing Thr or Gly at this position, results in the acquisition of resistance against methotrexate by extruding this compound from the cells (34). Because the amino acid at position 482 in our clone was Arg, the present results showing that Arg-482 ABCG2 transports methotrexate (Fig. 5) are consistent with the previous findings by Volk *et al.* (34). It would be noteworthy to point out the fact that the effective concentration of methotrexate to reduce the growth of ABCG2 overexpressing MCF/MX cells was much lower than the affinity of this drug toward ABCG2 (Table II); Volk *et al.* (34) reported that the IC_{50} values of methotrexate to reduce the cell growth were 0.10 and 11.3 μM for parental MCF7/WT and MCF7/MX cells, respectively.

In conclusion, ABCG2 was found to efficiently transport sulfate conjugates of steroids and xenobiotics such as E_1S, DHEAS, and 4-MUS. ABCG2 also accepts substrates for MRP1 and 2 (such as methotrexate, $E_2$17βG, and DNP-SG) to a much lesser extent compared with E_1S. It was suggested that ABCG2 preferentially transports sulfated conjugates and that E_1S and DHEAS are the potential physiological substrates for this transporter.

REFERENCES

1. Doyle, L. A., Yang, W., Abruzzo, L. V., Krogmann, T., Gao, Y., Rishi, A. K., and Ross, D. D. (1998) *Proc. Natl. Acad. Sci. U. S. A.* **95**, 15665–15670
2. Allikmets, R., Schriml, L. M., Hutchinson, A., Romano-Spica, V., and Dean, M.

(1998) *Cancer Res.* **58,** 5337–5339
3. Miyake, K., Mickley, L., Litman, T., Zhan, Z., Robey, R., Cristensen, B., Brangi, M., Greenberger, L., Dean, M., Fojo, T., and Bates, S. E. (1999) *Cancer Res.* **59,** 8–13
4. Scheffer, G. L., Maliepaard, M., Pijnenborg, A. C., van Gastelen, M. A., de Jong, M. C., Schroeijers, A. B., van der Kolk, D. M., Allen, J. D., Ross, D. D., van der Valk, P., Dalton, W. S., Schellens, J. H., and Scheper, R. J. (2000) *Cancer Res.* **60,** 2589–2593
5. Litman, T., Druley, T. E., Stein, W. D., and Bates, S. E. (2001) *Cell. Mol. Life Sci.* **58,** 931–959
6. Maliepaard, M., Scheffer, G. L., Faneyte, I. F., van Gastelen, M. A., Pijnenborg, A. C., Schinkel, A. H., van De Vijver, M. J., Scheper, R. J., and Schellens, J. H. (2001) *Cancer Res.* **61,** 3458–3464
7. Zhou, S., Schuetz, J. D., Bunting, K. D., Colapietro, A. M., Sampath, J., Morris, J. J., Lagutina, I., Grosveld, G. C., Osawa, M., Nakauchi, H., and Sorrentino, B. P. (2001) *Nat. Med.* **7,** 1028–1034
8. Zhou, S., Morris, J. J., Barnes, Y., Lan, L., Schuetz, J. D., and Sorrentino, B. P. (2002) *Proc. Natl. Acad. Sci. U. S. A.* **99,** 12339–12344
9. Jonker, J. W., Buitelaar, M., Wagenaar, E., Van Der Valk, M. A., Scheffer, G. L., Scheper, R. J., Plosch, T., Kuipers, F., Oude Elferink, R. P., Rosing, H., Beijnen, J. H., and Schinkel, A. H. (2002) *Proc. Natl. Acad. Sci. U. S. A.* **12,** 15649–15654
10. Jonker, J. W., Smit, J. W., Brinkhuis, R. F., Maliepaard, M., Beijnen, J. H., Schellens, J. H., and Schinkel, A. H. (2000) *J. Natl. Cancer Inst.* **92,** 1651–1656
11. König, J., Nies, A. T., Cui, Y., Leier, I., and Keppler, D. (1999) *Biochim. Biophys. Acta* **1461,** 377–394
12. Suzuki, H., and Sugiyama, Y. (1999) *Pharm. Biotechnol.* **12,** 387–439
13. Suzuki, H., and Sugiyama, Y. (2000) *Eur. J. Pharm. Sci.* **12,** 3–12
14. Borst, P., Evers, R., Kool, M., and Wijnholds, J. (2000) *J. Natl. Cancer Inst.* **92,** 1295–1302
15. Keppler, D., and Konig, J. (2000) *Semin. Liver Dis.* **20,** 265–272
16. Suzuki, H., and Sugiyama, Y. (1998) *Semin. Liver Dis.* **18,** 359–376
17. Takenaka, O., Horie, T., Kobayashi, K., Suzuki, H., and Sugiyama, Y. (1995) *Pharm. Res.* **12,** 1746–1755
18. Niinuma, K., Takenaka, O., Horie, T., Kobayashi, K., Kato, Y., Suzuki, H., and Sugiyama, Y. (1997) *J. Pharmacol. Exp. Ther.* **282,** 866–872
19. Qian, Y. M., Song, W. C., Cui, H., Cole, S. P., and Deeley, R. G. (2001) *J. Biol. Chem.* **276,** 6404–6411
20. Cui, Y., König, J., and Keppler, D. (2001) *Mol. Pharmacol.* **60,** 934–943
21. Akita, H., Suzuki, H., Ito, K., Kinoshita, S., Sato, N., Takikawa, H., and Sugiyama, Y. (2001) *Biochim. Biophys. Acta* **1511,** 7–16
22. Niinuma, K., Kato, Y., Suzuki, H., Tyson, C. A., Weizer, V., Dabbs, J. E., Froehlich, R., Green, C. E., and Sugiyama, Y. (1999) *Am. J. Physiol.* **276,** G1153–G1164
23. Kobayashi, K., Sogame, Y., Hara, H., and Hayashi, K. (1990) *J. Biol. Chem.* **265,** 7737–7741
24. Kage, K., Tsukahara, S., Sugiyama, T., Asada, S., Ishikawa, E., Tsuruo, T., and Sugimoto, Y. (2002) *Int. J. Cancer* **97,** 626–630
25. Hirohashi, T., Suzuki, H., and Sugiyama, Y. (1999) *J. Biol. Chem.* **274,** 15181–15185
26. Hirohashi, T., Suzuki, H., Chu, X. Y., Tamai, I., Tsuji, A., and Sugiyama, Y. (2000) *J. Pharmacol. Exp. Ther.* **292,** 265–270
27. Ozvegy, C., Litman, T., Szakacs, G., Nagy, Z., Bates, S., Varadi, A., and Sarkadi, B. (2001) *Biochem. Biophys. Res. Commun.* **285,** 111–117
28. Ozvegy, C., Varadi, A., and Sarkadi, B. (2002) *J. Biol. Chem.* **277,** 47980–47990
29. Borst, P., Evers, R., Kool, M., and Wijnholds, J. (1999) *Biochim. Biophys. Acta* **1461,** 347–357
30. Maliepaard, M., van Gastelen, M. A., de Jong, L. A., Pluim, D., van Waardenburg, R. C., Ruevekamp-Helmers, M. C., Floot, B. G., and Schellens, J. H. (1999) *Cancer Res.* **59,** 4559–4563
31. Litman, T., Brangi, M., Hudson, E., Fetsch, P., Abati, A., Ross, D. D., Miyake, K., Resau, J. H., and Bates, S. E. (2000) *J. Cell Sci.* **113,** 2011–2021
32. Nakatomi, K., Yoshikawa, M., Oka, M., Ikegami, Y., Hayasaka, S., Sano, K., Shiozawa, K., Kawabata, S., Soda, H., Ishikawa, T., Tanabe, S., and Kohno, S. (2001) *Biochem. Biophys. Res. Commun.* **288,** 827–832
33. Honjo, Y., Hrycyna, C. A., Yan, Q. W., Medina-Perez, W. Y., Robey, R. W., van de Laar, A., Litman, T., Dean, M., and Bates, S. E. (2001) *Cancer Res.* **61,** 6635–6639
34. Volk, E. L., Farley, K. M., Wu, Y., Li, F., Robey, R. W., and Schneider, E. (2002) *Cancer Res.* **62,** 5035–5040
35. Suzuki, M., Suzuki, H., Sugimoto, Y., and Sugiyama, Y. (2002) *Hepatology* **36,** 218A

Drug Metab. Pharmacokin. 18 (3): *SNP14* (212)-*SNP19* (217) (2003).

SNP Communication

Eight Novel Single Nucleotide Polymorphisms in ABCG2/BCRP in Japanese Cancer Patients Administered Irinotacan

Masaya ITODA[1], Yoshiro SAITO[1,2], Kuniaki SHIRAO[3], Hironobu MINAMI[4], Atsushi OHTSU[5], Teruhiko YOSHIDA[7], Nagahiro SAIJO[8], Hiroshi SUZUKI[9,*], Yuichi SUGIYAMA[9], Shogo OZAWA[1,6] and Jun-ichi SAWADA[1,2]

[1]*Project team for Pharmacogenetics,*
[2]*Division of Biochemistry and Immunochemistry,*
[6]*Division of Pharmacology, National Institute of Health Sciences, Tokyo, Japan*
[3]*Gastrointestinal Oncology Division,*
[8]*Medical Oncology Division, National Cancer Center Hospital,*
[7]*Genetics Division, National Cancer Center Research Institute, Tokyo, Japan*
[4]*Division of Oncology/Hematology,*
[5]*Division of GI Oncology/Digestive Endoscopy, National Cancer Center Hospital East, Chiba, Japan*
[9]*Graduate School of Pharmaceutical Sciences, The University of Tokyo, Tokyo, Japan*

Summary: Eight novel single nucleotide polymorphisms (SNPs) were found in the gene encoding the ATP-binding cassette transporter, *ABCG2/BCRP*, from 60 Japanese individuals administered the anti-cancer drug irinotecan. The detected SNPs were as follows:
1) SNP, MPJ6_AG2005 (IVS2−93T>C); Gene Name, *ABCG2*; Accession Number, NT_006204; 2) SNP, MPJ6_AG2007 (IVS3+71_72 insT); Gene Name, *ABCG2*; Accession Number, NT_006204; 3) SNP, MPJ6_AG2012 (IVS6−204C>T); Gene Name, *ABCG2*; Accession Number, NT_006204; 4) SNP, MPJ6_AG2015 (at nucleotide 1098G>A (exon 9) from the A of the translation initiation codon); Gene Name, *ABCG2*; Accession Number, NT_006204; 5) SNP, MPJ6_AG2017 (1291T>C (exon 11)); Gene Name, *ABCG2*; Accession Number, NT_006204; 6) SNP, MPJ6_AG2019 (IVS11−135G>A); Gene Name, *ABCG2*; Accession Number, NT_006204; 7) SNP, MPJ6_AG2020 (1465T>C (exon 12)); Gene Name, *ABCG2*; Accession Number, NT_006204; 8) SNP, MPJ6_AG2023 (IVS13+65T>G); Gene Name, *ABCG2*; Accession Number, NT_006204.
MPJ6_AG2015 was a synonymous SNP (E366E). MPJ6_AG2017 and MPJ6_AG2020 resulted in amino acid alterations, F431L and F489L, respectively.

Key words: *ABCG2*; novel SNP; amino acid alteration; ATP-binding cassette transporter

Introduction

The breast cancer resistance protein (BCRP) is the second reported G family member of the ATP-binding cassette (ABC) transporter.[1)] cDNAs encoding BCRP were isolated from human placenta[1)] and established cancer cell lines, which concomitantly showed resistance to a number of anti-cancer drugs, including SN-38, mitoxantrone, and topotecan.[2-5)] The *ABCG2* gene was mapped to chromosome 4q22.[6)] Immunohistochemistry using anti-BCRP antibodies revealed expression in placental syncytiotrophoblasts, small intestine and colon epithelium, the liver canalicular membrane, breast ducts and lobules, as well as veinous and capillary endothelium.[7)] The apical localization in the small intestine and colon epithelium is assumed to protect the tissues from intruding toxic xenobiotics.[7)] Therefore, it

On March 12, 2003, these SNPs were not found in "A database of Japanese Single Nucleotide Polymorphisms (http://snp.ims.u-tokyo.ac.jp/)", "dbSNP in the National Center for Biotechnology Information (http://www.ncbi.nlm.nih.gov/SNP/)", or "The Human Gene Mutation Database (http://archive.uwcm.ac.uk/uwcm/mg/hgmd0.html)". This study was supported in part by the Program for the Promotion of Fundamental Studies in Health Sciences (MPJ-1 and -6) of the Organization for Pharmaceutical Safety and Research (OPSR) of Japan.

Received; March 15, 2003, Accepted; May 6, 2003
To whom correspondence should be addressed: Shogo OZAWA, Ph.D., *Division of Pharmacology, National Institute of Health Sciences, 1-18-1, Kamiyoga, Setagaya-ku, Tokyo 158-8501, Japan. Tel. +81-3-3700-9737, Fax. +81-3-3707-6950, E-mail: sozawa@nihs.go.jp*
*Present address: Department of Pharmacy, The University of Tokyo, Tokyo, Japan

Table 1. PCR Primers used for the amplification of *ABCG2* exons in the present study

Exon	Primer name	Forward primer	Primer name	Reverse primer
1	ABCG2-1F	5′-CTGTGCCCACTCAAAAGGTT-3′	ABCG2-1R1	5′-GAAACTGCGAAAGGCTAAAA-3′
2	ABCG2-2F	5′-GGATGTTCTTATCACAATGG-3′	ABCG2-2R	5′-CAAATGAAAGCATGTGTCTG-3′
3	ABCG2-3F	5′-TGGTTTGTGCTTGTGTTCTA-3′	ABCG2-3R	5′-GCTCAATAAATACCTGCTCG-3′
4	ABCG2-4F	5′-GGATTCAAAGTAGCCATGAGAT-3′	ABCG2-4R	5′-GTCACATAATCAACTGGAAGCA-3′
5	ABCG2-5F	5′-GGCTTTGCAGACATCTATGGAG-3′	ABCG2-5R1	5′-CAGGTTAATTTCCACGTTCA-3′
6	ABCG2-6F	5′-ACCAGGTATCCACTTATTTG-3′	ABCG2-6R	5′-TGACTTTCACTCCAACAGAA-3′
7	ABCG2-7F2	5′-AAGACTGTCCTAGAATCTGC-3′	ABCG2-7R	5′-TAGCACCAAATGGAACAAAC-3′
8	ABCG2-8F2	5′-ATTACATGGGAAGAAGAGAG-3′	ABCG2-8R	5′-TTGACTGGTATCAGAAGACTG-3′
9	ABCG2-9F4	5′-TAGAATGAAGGTGTTAGGGA-3′	ABCG2-9R1	5′-AGGTGGAGTGAAGATAACAA-3′
10	ABCG2-10F	5′-GCCAAGCCATTGAGTGTTTA-3′	ABCG2-10R1	5′-CTGACTCATCCTACCCTCAA-3′
11	ABCG2-11F1	5′-ACCAGAACAGTTTCCCTTTT-3′	ABCG2-11R	5′-AAAAGTACTGGTAATCCTCCG-3′
12	ABCG2-12F1	5′-TCATGGGATGCTTTCTCAGG-3′	ABCG2-12R	5′-GTGTTTCCTTATCTCATGGT-3′
13	ABCG2-13F	5′-CATGGACAGACACAACATTG-3′	ABCG2-13R	5′-GGCAAAGAGGAAAGTTAGTA-3′
14	ABCG2-14F2	5′-ACCGTAAATGACTTCAGCTA-3′	ABCG2-14R2	5′-ATTCTCATTCCTTGCTCCTA-3′
15	ABCG2-15F1	5′-TTGGTGAGACAAAGACTGTG-3′	ABCG2-15R1	5′-GCAGCAGAATACTGAGGGGT-3′
16	ABCG2-16F	5′-AGGCTTGGTTCAATTTTAGG-3′	ABCG2-16R	5′-CATGATGTCTTGGGTTCTTT-3′

would be possible that *ABCG2/BCRP* genetic polymorphisms would affect disposition of irinotecan and its metabolites.

Information on *ABCG2/BCRP* single nucleotide polymorphisms (SNPs) has been published.[8-10] Five naturally occurring nonsynonymous SNPs have been reported in Japanese and Caucasians: V12M, Q126Stop, Q141K, I206L, and N590Y.[8-10] SNP Q126Stop was found in 3 out of 124 healthy Japanese subjects.[9] Since it may be possible that *ABCG2/BCRP* polymorphisms are associated with the effectiveness and adverse effects of irinotecan, *ABCG2/BCRP* exons and their flanking regions were sequenced to identify Japanese specific SNPs. We found eight novel SNPs from the analysis of 60 Japanese individuals administered irinotecan for cancer treatment.

Materials and Methods

Human genomic DNA samples: All 60 Japanese subjects were administered irinotecan for cancer treatment. Genomic DNA extracted from blood leukocytes was used as template for DNA sequencing. The ethics committees of both the National Cancer Center and the National Institute of Health Sciences approved this study. Written informed consent was obtained from all participating subjects.

***ABCG2/BCRP* polymerase chain reaction (PCR) conditions and sequencing:** We sequenced all 16 *ABCG2/BCRP* exons after performing a single PCR amplification reaction (50 μL) using multiplex primer sets (**Table 1**) that could amplify all *ABCG2/BCRP* exons from genomic DNA (400 ng). Primers were located in the introns near the exon-intron boundaries. The amplification was done with primers (0.5 μM each) and Ex-Taq DNA polymerase (0.625 U, TaKaRa Co., Kyoto, Japan) in the presence of 0.8 mM dNTPs using the GeneAmp PCR system 9700 (Perkin-Elmer Co., CT). Then, each exon was individually amplified by a second PCR round with the same primer sets (**Table 1**) with conditions identical to the primary PCR, except for the 50 μL total volume. Sequencing was performed on both strands using primers listed in **Table 2** with an ABI BigDye Terminator Cycle Sequencing Kit version 3 (Applied Biosystems, Foster City, CA). The dye-incorporated DNA fragments were analyzed on an ABI Prism 3700 DNA Analyzer (Applied Biosystems).

Results and discussion: Disposition of irinotecan and its efficacy may be influenced by genetic polymorphisms of irinotecan-metabolizing enzymes and transporters including *ABCG2/BCRP*. In this study, we analyzed *ABCG2/BCRP* sequences for genetic polymorphisms in Japanese individuals who suffered from various cancers and who were administered irinotecan.

The *ABCG2/BCRP* PCR conditions have been shown to be specific for *ABCG2/BCRP* since all the nucleotide sequences of the PCR-amplified DNA were identical to those of the *ABCG2/BCRP* reference sequence (NT_006204), except for the SNPs described below:

1) SNP, MPJ6_AG2005; Gene Name, *ABCG2*; Accession Number, NT_006204; Length, 25 bases; 5′-TTTGTAATTTCAT/CCAACCTTCATTG-3′

2) SNP, MPJ6_AG2007; Gene Name, *ABCG2*; Accession Number, NT_006204; Length, 25 bases; 5′-CCACTTTTTTTT-/TGTGTGCGAGCAG-3′

3) SNP, MPJ6_AG2012; Gene Name, *ABCG2*; Accession Number, NT_006204; Length, 25 bases; 5′-TTGTCAATACAAC/TACACTGAAAATT-3′

4) SNP, MPJ6_AG2015; Gene Name, *ABCG2*; Accession Number, NT_006204; Length, 25 bases; 5′-AGTCTTCAAGGAG/AATCAGCTACACC-3′

5) SNP, MPJ6_AG2017; Gene Name, *ABCG2*;

Table 2. Primers used for sequencing *ABCG2* exons

Exon	Primer name	Forward primer	Primer name	Reverse primer
1	ABCG2-1F1	5′-GTGCCCACTCAAAAGGTTCC-3′	ABCG2-1R	5′-CTAAAAAACTCAGTCGTCTCGT-3′
2	ABCG2-2F	5′-GGATGTTCTTATCACAATGG-3′	ABCG2-2R	5′-CAAATGAAAGCATGTGTCTG-3′
3	ABCG2-3F1	5′-GGTTTGTGCTTGTGTTCTAT-3′	ABCG2-3R	5′-GCTCAATAAATACCTGCTCG-3′
4	ABCG2-4F	5′-GGATTCAAAGTAGCCATGAGAT-3′	ABCG2-4R	5′-GTCACATAATCAACTGGAAGCA-3′
5	ABCG2-5F1	5′-CTTTGCAGACATCTATGGAGT-3′	ABCG2-5R	5′-GACCATACACATTACAGGAAAC-3′
6	ABCG2-6F1	5′-TGTCTCTTACAGGACTGGCA-3′	ABCG2-6R	5′-TGACTTTCACTCCAACAGAA-3′
7	ABCG2-7F3	5′-GACAAAGTCAGGCTGAACTA-3′	ABCG2-7R1	5′-CTACCCAAAGACCAAACAGC-3′
8	ABCG2-8F	5′-TCTGTCTTCTCTAGCCTTACC-3′	ABCG2-8R2	5′-ACAGAAATTCACAAAGCCAC-3′
9	ABCG2-9F3	5′-CATCCAAGAAAGGGTTCACA-3′	ABCG2-9R	5′-AAGGGTGGGTAGAAGATAAA-3′
10	ABCG2-10F1	5′-CAAGCCATTGAGTGTTTATC-3′	ABCG2-10RS	5′-GAATGACATTTACACTATACTTG-3′
11	ABCG2-11F	5′-CCCTTTTTTTCCTGCTTAAC-3′	ABCG2-11R2	5′-AACCCCAGATGTAATCAGTC-3′
12	ABCG2-12F	5′-CTGTCAGCAGAGGTCTGTAAC-3′	ABCG2-12R1	5′-TTCCTTATCTCATGGTTTGG-3′
13	ABCG2-13F1	5′-GGACAGACACAACATTGGAG-3′	ABCG2-13R1	5′-AAGTAAAGCAGAGCCCCATT-3′
14	ABCG2-14F1	5′-TGCAGAGGAGAAGAGTTTAG-3′	ABCG2-14R	5′-TTCTGGATGGGAGACTTTCA-3′
15	ABCG2-15FS	5′-AGACAAAGACTGTGAATATGTT-3′	ABCG2-15R2	5′-AGCAGAATACTGAGGGGTTG-3′
16	ABCG2-16F1	5′-GCTTGGTTCAATTTTAGGCT-3′	ABCG2-16R1	5′-GATGGCAAGGGAACAGAAAA-3′

Table 3. Novel SNPs in the *ABCG2* gene found in Japanese individuals

SNP name	AG2005	AG2007	AG2012	AG2015	AG2017	AG2019	AG2020	AG2023
	Intron 2	**Intron 3**	**Intron 6**	**Exon 9**	**Exon 11**	**Intron 11**	**Exon 12**	**Intron 13**
Position (cDNA)	IVS2−93[a]	IVS3+71_72 insT[b]	IVS6−204	1098	1291	IVS11−135	1465	IVS13+65
Nucleotide	T>C	->T	C>T	G>A	T>C	G>A	T>C	T>G
Amino acid				E366E	F431L		F489L	
Frequency, %	T:97.5	-:99.2	C:96.7	G:99.2	T:99.2	G:98.3	T:99.2	G:99.2
	C:2.5	T:0.8	T:3.3	A:0.8	C:0.8	A:1.7	C:0.8	A:0.8

[a] Numbers following IVS (intervening sequence) represents number of the preceding exon. In the case of end of the intron, the SNP position is expressed by a minus sign and the bases upstream of the next exon.

[b] Numbers following IVS represents number of the preceding exon. In the case of beginning of the intron, the SNP position is expressed by a plus sign and the bases downstream of the preceding exon. In IVS3+71_72 insT, "insT" stands for insertion of a "T". Minus sign>T, "->T", represents insertion of a "T" at the position between nucleotides 71 and 72.

Accession Number, NT_006204; Length, 25 bases; 5′-GCTGGGGTTCTCT/CTCTTCCTGACGA-3′

6) SNP, MPJ6_AG2019; Gene Name, *ABCG2*; Accession Number, NT_006204; Length, 25 bases; 5′-CATGCATAGTGGG/ATCTAGCCCTGAG-3′

7) SNP, MPJ6_AG2020; Gene Name, *ABCG2*; Accession Number, NT_006204; Length, 25 bases; 5′-CCAAGTATTATAT/CTTACCTGTATAG-3′

8) SNP, MPJ6_AG2023; Gene Name, *ABCG2*; Accession Number, NT_006204; Length, 25 bases; 5′-CTTCCTGCACATT/GCACTTGTCATGT-3′.

SNP frequencies are summarized in **Table 3.** The electropherograms of the novel SNPs that were found in only one subject are shown in **Fig. 1.** Of these SNPs, two SNPs, MPJ6_AG2017 and 020, that were each found in 1 subject, introduced nonsynonymous amino acid changes (F431L and F489L), respectively. Honjo *et al.* recently reported that R482T and R482G variants were found in cells after drug selection.[11] ABCG2-ATPase activity was influenced by amino acid residue 482,[12] which might be located within the transmembrane domain.[10] Currently, the functional significance of these SNPs is unknown; however, the clinical outcome of those who have these non-synonymous SNPs should carefully be evaluated.

Consistent with a previous report,[9] we also found 2 patients who had a heterozygous Q126Stop SNP. This nonsense variant should be evaluated in conjunction with the clinical outcome. Since irinotecan was administered by infusion in these subjects, *ABCG2* genetic polymorphism might have effects on the drug resistance of cancerous tissues and on adverse reactions related to biliary excretion of irinotecan and SN-38 to the intestine in consideration of its expression in bile canaliculi, and intestinal and colon epithelium. In this study, we found 8 novel SNPs including 2 non-synonymous SNPs in *ABCG2/BCRP* in 60 irinotecan-administered Japanese patients. Our data will be useful for detailed identifica-

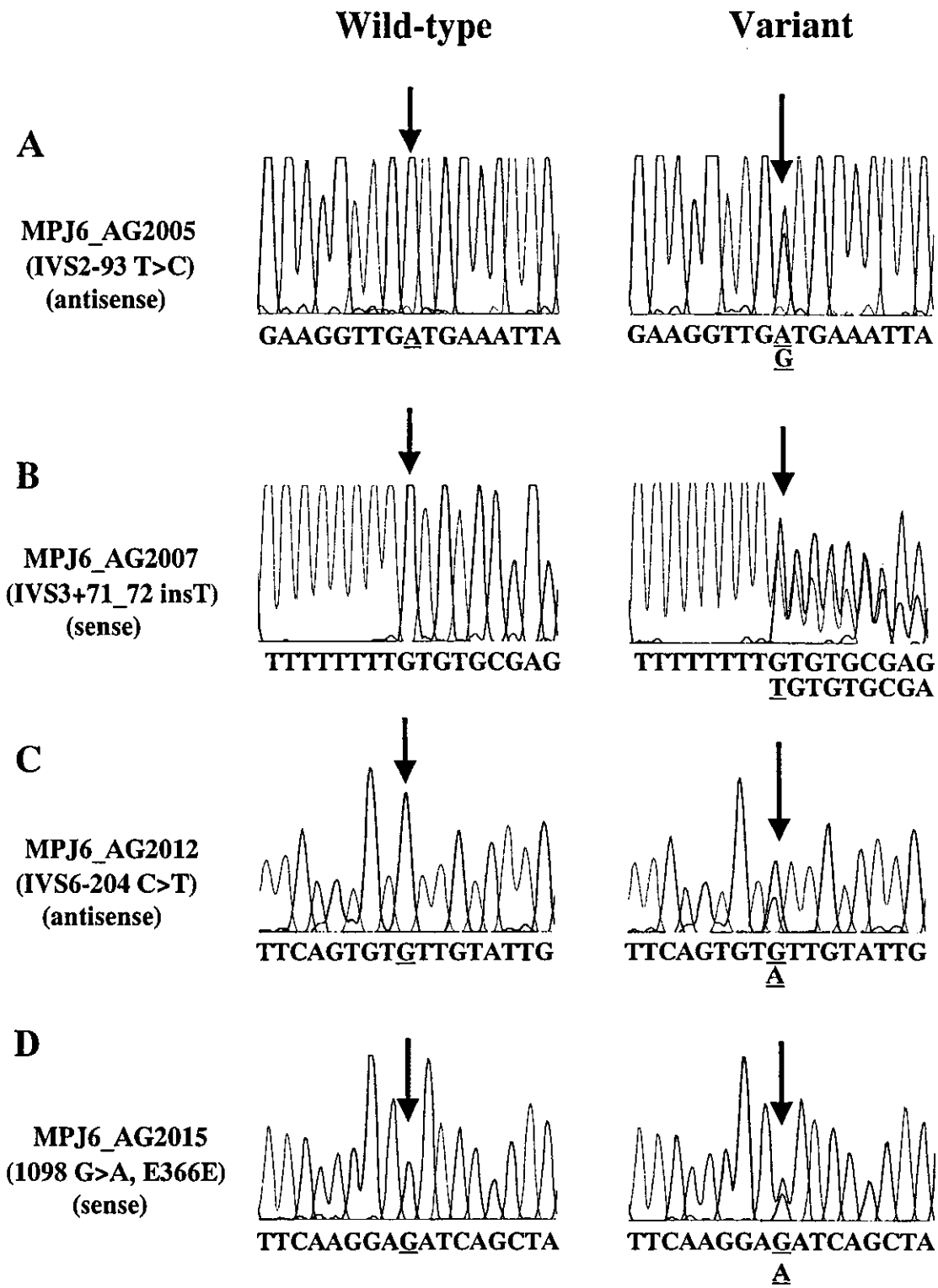

Fig. 1 (A–D). Electropherograms for the *ABCG2/BCRP* SNPs found in this study.
(A) Homozygous wild-type and wild-type/IVS2−93T>C (MPJ6_G2005). (B)Homozygous wild-type and wild-type/IVS3+71_72 insT (MPJ6_G2007). (C) Homozygous wild-type and wild-type/IVS6−204C>T (MPJ6_G2012). (D) Homozygous wild-type and wild-type/1098G>A (MPJ6_G2015). (E) Homozygous wild-type and wild-type/1291T>C (F431L) (MPJ6_G2017). (F) Homozygous wild-type and wild-type/IVS11−135G>A (MPJ6_G2019). (G) Homozygous wild-type and wild-type/1465T>C (F489L) (MPJ6_G2020). (H) Homozygous wild-type and wild-type/IVS13+65T>G (MPJ6_G2023).
Arrows indicate the SNP location. In the electropherograms, A, C, G, and T are colored green, blue, black, and red, respectively.

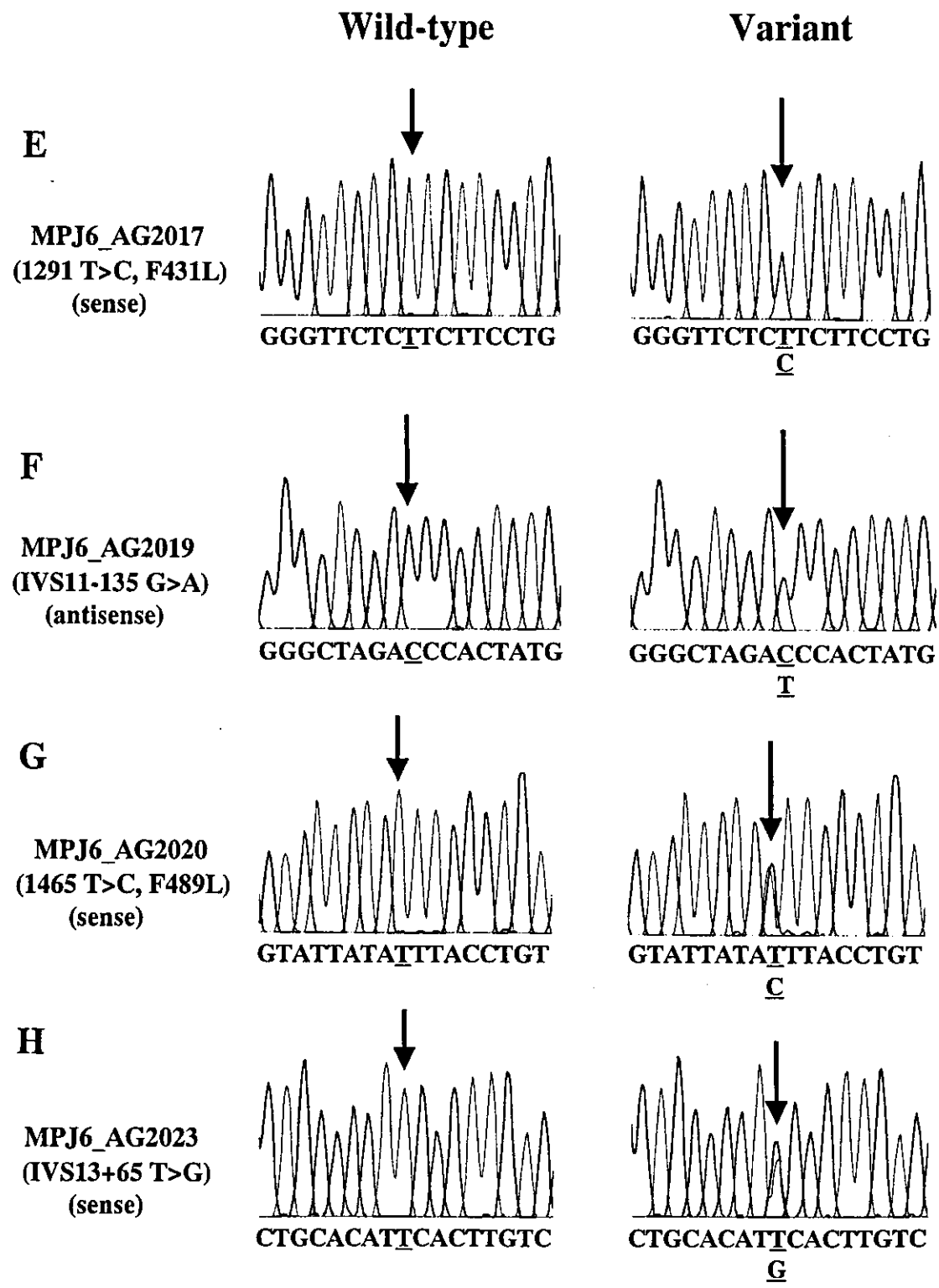
Wild-type
Variant
E
MPJ6_AG2017
(1291 T>C, F431L)
(sense)
GGGTTCTCTTCTTCCTG
GGGTTCTCTTCTTCCTG
C
F
MPJ6_AG2019
(IVS11-135 G>A)
(antisense)
GGGCTAGACCCACTATG
GGGCTAGACCCACTATG
T
G
MPJ6_AG2020
(1465 T>C, F489L)
(sense)
GTATTATATTTACCTGT
GTATTATATTTACCTGT
C
H
MPJ6_AG2023
(IVS13+65 T>G)
(sense)
CTGCACATTCACTTGTC
CTGCACATTCACTTGTC
G

Fig. 1 (E–H).

tion of *ABCG2/BCRP* haplotypes in conjunction with other frequently found SNPs, including non-synonymous ones (34G>A (V12M, SNP frequency 19%) and 421C>A (Q141K, SNP frequency 33%)) in the Japanese population. These non-synonymous SNPs were not apparently linked to each other. MPJ6_AG2012 was closely associated with the known SNP, IVS1-99G>A (rs1584481, ssj0001922), but not with the SNPs, 34G>A (V12M) and 421C>A (Q141K). A pharmacogenetic study on *ABCG2/BCRP* for irinotecan-administered patients is currently undergoing.

Acknowledgments: We thank Ms. Chie Knudsen for her secretarial assistance.

References

1) Allikmets, R., Schriml, L. M., Hutchinson, A., Romano-Spica, V. and Dean, M.: A human placenta-specific ATP-binding cassette gene (ABCP) on chromosome 4q22 that is involved in multidrug resistance. *Cancer Res.*, **58**, 5337–5339 (1998).
2) Doyle, L. A., Yang, W., Abruzzo, L. V., Krogmann, T., Gao, Y., Rishi, A. K. and Ross, D. D.: A multidrug resistance transporter from human MCF-7 breast cancer cells. *Proc. Natl. Acad. Sci.*, **95**, 15665–15670 (1998).
3) Maliepaard, M., van Gastelen, M. A., de Jong, L. A., Pluim, D., van Waardenburg, R. C. A. M., Ruevekamp-Helmers, M. C., Floot, B. G. and Schellens, J. H. M.: Overexpression of BCRP/MXR/ABCP gene in a topotecan-selected ovarian tumor cell line. *Cancer Res.*, **59**, 4559–4563 (1999).
4) Kawabata, S., Oka, M., Shiozawa, K., Tsukamoto, K., Nakatomi, K., Soda, H., Fukuda, M., Ikegami, Y., Sugahara, K., Yamada, Y., Kamihira, S., Doyle, L. A., Ross, D. D. and Kohno, S.: Breast cancer resistance protein directly confers SN-38 resistance of lung cancer cells. *Biochem. Biophys. Res. Commun.*, **280**, 1216–1223 (2001).
5) Litman, T., Brangi, M., Hudson, E., Fetsch, P., Abati, A., Ross, D. D., Miyake, K., Resau, J. H. and Bates, S. E.: The multidrug-resistant phenotype associated with overexpression of the new ABC half-transporter, MXR (ABCG2). *J. Cell. Sci.*, **113**, 2011–2021 (2000).
6) Allikmets, R., Gerrard, B., Hutchinson, A. and Dean, M.: Characterization of the human ABC superfamily: isolation and mapping of 21 new genes using the expressed sequence tags database. *Human Mol. Genet.*, **5**, 1649–1655 (1996).
7) Maliepaard, M., Scheffer, G. L., Faneyte, I. F., van Gastelen, M. A., Pijnenborg, A. C. L. M., Schinkel, A. H., van de Vijver, M. J., Scheper, R. J. and Schellens, J. H. M.: Subcellular localization and distribution of the breast cancer resistance protein transporter in normal human tissues. *Cancer Res.*, **61**, 3458–3464 (2001).
8) Iida, A., Saito, S., Sekine, A., Mishima, C., Kitamura, Y., Kondo, K., Harigae, S., Osawa, S. and Nakamura, Y.: Catalog of 605 single-nucleotide polymorphisms (SNPs) among 13 genes encoding human ATP-binding cassette transporters: *ABCA4*, *ABCA7*, *ABCA8*, *ABCD1*, *ABCD3*, *ABCD4*, *ABCE1*, *ABCF1*, *ABCG1*, *ABCG2*, *ABCG4*, *ABCG5*, and *ABCG8*. *J. Hum. Genet.*, **47**, 285–310 (2002).
9) Imai, Y., Nakane, M., Kage, K., Tsukahara, S., Ishikawa, E., Tsuruo, T., Miki, Y. and Sugimoto, Y.: C421A polymorphism in the human breast cancer resistance protein gene is associated with low expression of Q141K protein and low-level drug resistance. *Mol. Cancer Ther.*, **1**, 611–616 (2002).
10) Zamber, C. P., Lamba, J. K., Yasuda, K., Farnum, J., Thummel, K., Schuetz, J. D. and Schuetz, E. G.: Natural allelic variants of breast cancer resistance protein (BCRP) and their relationship to BCRP expression in human intestine. *Pharmacogenetics*, **13**, 19–28 (2003).
11) Honjo, Y., Hrycyna, C. A., Yan, Q. W., Medina-Perez, W. Y., Robey, R. W., van de Laar, A., Litman, T., Dean, M. and Bates, S. E.: Acquired mutations in the *MXR/BCRP/ABCP* gene alter substrate specificity in *MXR/BCRP/ABCP*-overexpressing cells. *Cancer Res.*, **61**, 6635–6639 (2001).
12) Ozvegy, C., Varadi, A. and Sarkadi, B.: Characterization of drug transport, ATP hydrolysis, and nucleotide trapping by the human *ABCG2* multidrug transporter. Modulation of substrate specificity by a point mutation. *J. Biol. Chem.*, **277**, 47980–47990 (2002).

THE JOURNAL OF BIOLOGICAL CHEMISTRY
Vol. 278, No. 44, Issue of October 31, pp. 43489–43495, 2003
Printed in U.S.A.

Functional Characterization of Rat Brain-specific Organic Anion Transporter (Oatp14) at the Blood-Brain Barrier

HIGH AFFINITY TRANSPORTER FOR THYROXINE*

Received for publication, June 30, 2003
Published, JBC Papers in Press, August 15, 2003, DOI 10.1074/jbc.M306933200

Daisuke Sugiyama‡, Hiroyuki Kusuhara‡, Hirokazu Taniguchi§, Shumpei Ishikawa§, Yoshitane Nozaki‡, Hiroyuki Aburatani§, and Yuichi Sugiyama‡¶

From the ‡Graduate School of Pharmaceutical Sciences, The University of Tokyo, 7-3-1 Hongo, Bunkyo-ku, Tokyo 113-0033, Japan and §Research Center for Advanced Science and Technology, The University of Tokyo, 4-6-1 Komaba, Meguro-ku, Tokyo 153-8904, Japan

Oatp14/blood-brain barrier-specific anion transporter 1 (*Slc21a14*) is a novel member of the organic anion transporting polypeptide (Oatp/OATP) family. Northern blot analysis revealed predominant expression of Oatp14 in the brain, and Western blot analysis revealed its expression in the brain capillary and choroid plexus. Immunohistochemical staining indicated that Oatp14 is expressed in the border of the brain capillary endothelial cells. When expressed in human embryonic kidney 293 cells, Oatp14 transports thyroxine (T_4; prothyroid hormone) (K_m = 0.18 μM), as well as amphipathic organic anions such as 17β estradiol-D-17β-glucuronide (K_m = 10 μM), cerivastatin (K_m = 1.3 μM), and troglitazone sulfate (K_m = 0.76 μM). The uptake of triiodothyronine (T_3), an active form produced from T_4, was significantly greater in Oatp14-expressed cells than in vector-transfected cells, but the transport activity for T_3 was ~6-fold lower that for T_4. The efflux of T_4, preloaded into the cells, from Oatp14-expressed cells was more rapid than that from vector-transfected cells (0.032 *versus* 0.006 min^{-1}). Therefore, Oatp14 can mediate a bidirectional transport of T_4. Sulfobromophthalein, taurocholate, and estrone sulfate were potent inhibitors for Oatp14, whereas digoxin, *p*-aminohippurate, or leukotriene C_4, or organic cations such as tetraetheylammonium or cimetidine had no effect. The expression levels of Oatp14 mRNA and protein were up- and down-regulated under hypo- and hyperthyroid conditions, respectively. Therefore, it may be speculated that Oatp14 plays a role in maintaining the concentration of T_4 and, ultimately, T_3 in the brain by transporting T_4 from the circulating blood to the brain.

Brain capillary endothelial cells are characterized by tightly sealed cellular junctions (tight junctions) and the paucity of fenestra and pinocytotic vesicles, which prevent free exchange between brain and blood (1, 2). Therefore, the uptake of nutrients by the brain occurs through the brain capillary endothelial cells via specific transport systems (3–7). Metabolic enzymes and efflux transporters expressed in the brain capillaries facilitate the elimination of endogenous wastes and xenobiotics from the brain, and restrict their brain accumulation (3–7). Because of these characteristics, the brain capillaries are referred to as the blood-brain barrier (BBB).[1]

The organic anion transporting polypeptides (Oatps in rodents and OATPs in human) belong to the growing gene family of organic anion/prostaglandin transporters that can mediate sodium-independent membrane transport of numerous endogenous and xenobiotic amphipathic compounds (8, 9). Fourteen members of the *Oatp/OATP* gene family have been identified in rodents and humans, and they are classified within the gene superfamily of solute carriers as the *Slc21a/SLC21A* gene family (Human Gene Nomenclature Committee DataBase) (8, 9). Several members of the Oatp/OATP family have been identified in the brain (Oatp1–3 and moat1 in rodents and OATP-A in human) (10–14). Especially, in the BBB, rat Oatp2 and human OATP-A have been shown to be expressed in the plasma membrane of the brain capillary endothelial cells (15, 16). Involvement of rat Oatp2 in the uptake and efflux transport of its substrates was investigated *in vivo* (17, 18). The uptake of [D-penicillamine^{2,5}]-enkephalin (DPDPE) from the blood to the brain was determined by the brain perfusion technique in the presence and absence of Oatp2 inhibitors (17). The brain uptake of DPDPE was increased in Mdr1a (P-glycoprotein) gene knockout mice, and the uptake in Mdr1a knockout mice was inhibited by the substrates and inhibitors of rat Oatp2 such as digoxin and 17β estradiol-D-17β-glucuronide ($E_2$17βG). Vice versa, when $E_2$17βG was microinjected into the cerebral cortex, the subsequent elimination of $E_2$17βG from the brain was carrier-mediated (18), and the elimination of $E_2$17βG was completely inhibited by co-administration of taurocholate and probenecid, whereas digoxin had only a partial effect (18). Partial inhibition by digoxin suggested that additional efflux transport system(s) for $E_2$17βG, which is taurocholate- and probenecid-sensitive, is involved in the brain capillary.

Li *et al.* (19) recently identified BBB-specific anion trans-

* This work was supported by grants-in-aid from the Ministry of Health, Labor and Welfare of Japan. The costs of publication of this article were defrayed in part by the payment of page charges. This article must therefore be hereby marked "*advertisement*" in accordance with 18 U.S.C. Section 1734 solely to indicate this fact.

¶ To whom correspondence should be addressed: Dept. of Molecular Pharmacokinetics, Graduate School of Pharmaceutical Sciences, The University of Tokyo, 7-3-1 Hongo, Bunkyo-ku, Tokyo 113-0033, Japan. Tel.: 81-3-5841-4770; Fax: 81-3-5841-4766; E-mail: sugiyama@mol.f.u-tokyo.ac.jp.

[1] The abbreviations used are: BBB, blood-brain barrier; Oatp, organic anion transporting polypeptide; BSAT, BBB-specific anion transporter; HEK293, human embryonic kidney 293; CA, cholate; GCA, glycocholate; LCA, lithocholate; CDCA, chenodeoxycholate; UDCA, ursodeoxycholate; PGD_2, prostaglandin D_2; PGE_2, prostaglandin E_2; E3040, 6-hydroxy-5,7-dimethyl-2-methylamino-4-(3-pyridylmethyl) benzothiazole; PBS, phosphate-buffered saline; DPDPE, [D-penicillamine^{2,5}]-enkephalin; $E_2$17βG, 17β estradiol-D-17β-glucuronide; T_4, thyroxine; TLCS, taurolithocholate sulfate; 4-MUS, 4-methylumbelliferone sulfate; TRO-S, troglitazone sulfate; RT, reverse transcriptase; MMI, methimazole; T_3, triiodothyronine; ES, estrone sulfate; BSP, sulfobromophthalein; LT, leukotriene; D2, type 2 iodothyronine deiodinase.

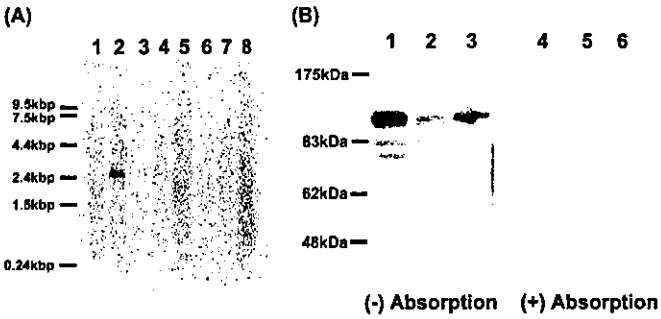

FIG. 1. **Tissue distribution of Oatp14.** *A*, Northern blotting. Commercially available rat multiple tissue Northern blots containing 2 μg of poly(A)$^+$ RNA was hybridized for 3 h using the Oatp14 fragment as a probe. *Lane 1*, heart; *lane 2*, brain; *lane 3*, spleen; *lane 4*, lung; *lane 5*, liver; *lane 6*, skeletal muscle; *lane 7*, kidney; *lane 8*, testis. *B*, Western blotting. Choroid plexus (*lanes 1* and *4*, 50 μg), brain homogenate (*lanes 2* and *5*, 50 μg), and isolated brain capillary (*lanes 3* and *6*, 50 μg) were separated by SDS-PAGE (10% separating gel). Oatp14 was detected by anti-Oatp14 polyclonal antibody.

porter 1 (BSAT1) using gene microarray techniques by comparing the gene expression profile of cDNA from the brain capillary with that from the liver and kidney. BSAT1 cDNA consisted of 2148 bp that encoded a 716-amino acid residues protein with 12 putative membrane-spanning domains. BSAT1 was highly enriched in the brain capillary compared with brain homogenate, liver, and kidney. Comparison of the cDNA sequences of BSAT1 revealed that it is the 14th member of the Oatp/OATP family (Oatp14). Although the localization at the BBB and the substrates of this isoform remain unknown, BBB-specific expression prompted us to hypothesize that Oatp14 accounts for the efflux of organic anions including $E_2 17\beta G$ via the BBB, together with Oatp2. The purpose of the present study is to characterize the substrate specificity and spectrum of inhibitors of Oatp14, as well as its tissue distribution and localization. Through this study, we found out that thyroxine (T_4) is a good substrate of Oatp14, and the expression level of Oatp14 in the BBB is affected by plasma thyroid conditions. The results of the present study suggest that Oatp14 plays an important role in regulating the concentration of T_4 in the central nervous system and in brain development.

EXPERIMENTAL PROCEDURES

Chemicals—[^{3}H]Leu-enkephalin was purchased from American Radiolabeled Chemicals (St. Louis, MO). [^{3}H]Pravastatin was kindly donated from Sankyo (Tokyo, Japan), [^{14}C]cerivastatin was from Bayer AG (Wuppertal, Germany), and [^{14}C]E3040 glucuronide and [^{14}C]E3040 sulfate were from Eisai (Tokyo, Japan). [^{3}H]Taurolithocholate sulfate (TLCS), [^{35}S]4-methylumbelliferone sulfate (4-MUS), and [^{35}S]troglitazone sulfate (TRO-S) were synthesized according to a method described previously (20, 21). The radiochemical purity of [^{3}H]TLCS, [^{35}S]4-MUS, and [^{35}S]TRO-S prepared by this method were more than 95%. Other labeled compounds were purchased from PerkinElmer Life Science. Unlabeled pravastatin, troglitazone, and its conjugated metabolites were kindly donated from Sankyo, unlabeled cerivastatin was from Bayer AG, and unlabeled E3040 glucuronide and E3040 sulfate were from Eisai. All other chemicals were commercially available, of reagent grade, and were used without any purification.

Capillary Isolation—Rat brain capillaries were isolated using a modification of the procedure of Boado *et al.* (22). All steps in the isolation procedure were carried out at 4 °C in pregassed (95% O_2-5% CO_2) solutions. Briefly, pieces of gray matter were gently homogenized in three volumes (v/w) of an artificial extracellular fluid buffer and, after addition of dextran (final concentration 15%), the homogenate was centrifuged at low speed. The resulting pellet was resuspended in Buffer B (103 mM NaCl, 25 mM $NaHCO_3$, 10 mM D-glucose, 4.7 mM KCl, 2.5 mM $CaCl_2$, 1.2 mM $MgSO_4$, 1.2 mM K_2HPO_4, and 15 mM HEPES, 1 mM sodium pyruvate, 0.5% (w/v) bovine serum albumin, pH 7.4) and then filtered through a 200-μm nylon mesh. The filtrate was passed over a column of glass beads, and after washing with Buffer B, the capillaries adhering to the beads were collected by gentle agitation.

FIG. 2. **Immunohistochemical staining of Oatp14 for brain slices.** Frozen sections of rat brain were used for immunohistochemical detection with peroxidase to probe for Oatp14 with a polyclonal antibody. The *lined* and *dotted arrows* represent luminal and abluminal sides of brain capillary endothelial cells, respectively. Positive labeling was only found in the border of brain capillary endothelial cells.

Northern Blot Analysis—A commercially available hybridization blot containing poly(A)$^+$ RNA from various rat tissues (rat multi-tissue Northern blot; Clontech) was used for the Northern blot analysis. A fragment (position numbers 1–807) from Oatp14 was used as a probe, and its nucleotide sequence showed less than 60% identity with other members of the Oatp family. The master blot filter was hybridized with the ^{32}P-labeled probe at 68 °C according to manufacturer's instructions. The filter was washed finally under high stringency conditions (0.1× SSC (1× SSC = 0.15 M NaCl and 0.015 M sodium citrate)) and 0.1% SDS at 65 °C and then exposed to Fuji imaging plates (Fuji Photo Film, Kanagawa, Japan) for 3 h at room temperature and examined using an imaging analyzer (BAS 2000; Fuji Photo Film).

Western Blot Analysis—Antiserum against Oatp14 was raised in rabbits against a synthetic peptide consisting of the 17 carboxyl-terminal amino acids of Oatp14. Antiserum was purified by affinity column chromatography using the antigen and used for subsequent analyses. Choroid plexus, brain homogenate, and isolated brain capillary samples were diluted with Loading Buffer (BioLabs, Hertfordshire, United Kingdom). They were then boiled for 3 min and loaded onto an 8.5% SDS-polyacrylamide electrophoresis gel with a 3.75% stacking gel. Proteins were electroblotted onto a polyvinylidene difluoride membrane (Pall Filtran, Karlstein, Germany) using a blotter (Trans-blot; Bio-Rad) at 15 V for 1 h. The membrane was blocked with TBS-T (Tris-buffered

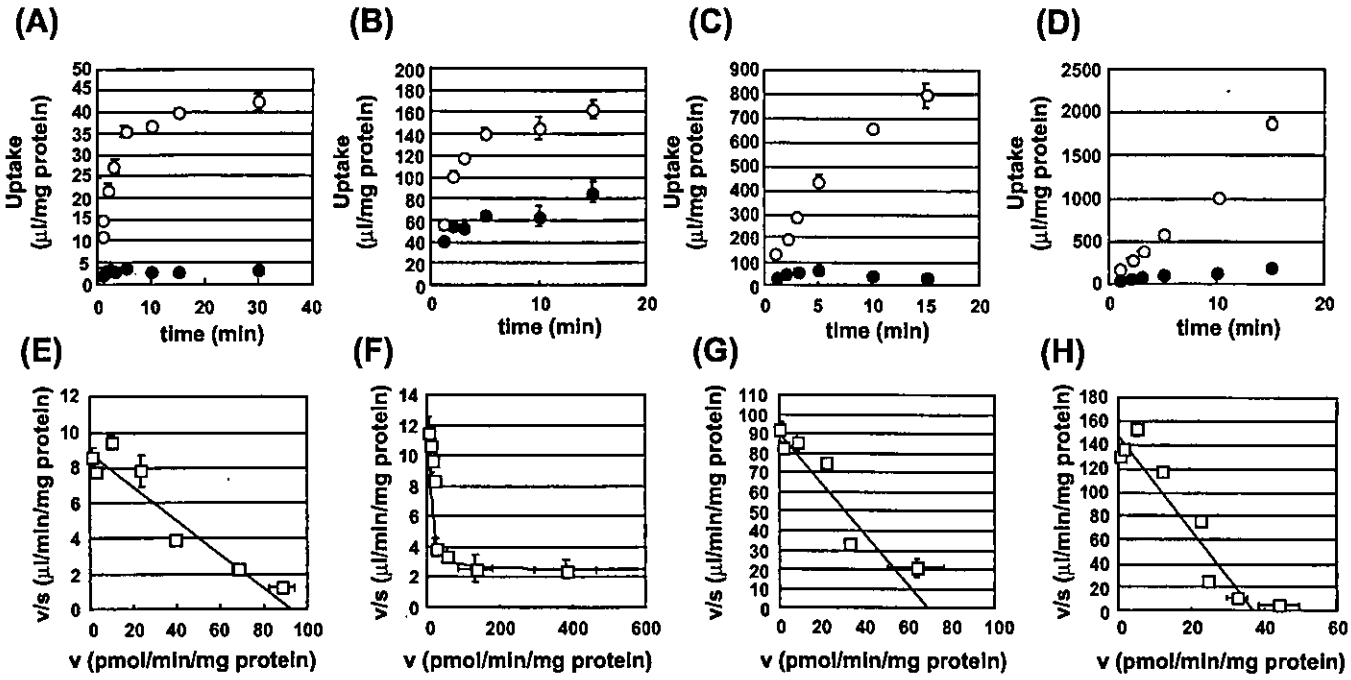

FIG. 3. **Time profiles and concentration dependence of the uptake of [^{3}H]$E_2$17βG, [^{14}C]cerivastatin, [^{35}S]TRO-S, and [^{125}I]T_4 by Oatp14-transfected HEK293 cells.** The uptake of [^{3}H]$E_2$17βG (*A* and *E*), [^{14}C]cerivastatin (*B* and *F*), [^{35}S]TRO-S (*C* and *G*), and [^{125}I]T_4 (*D* and *H*) by Oatp14-transfected HEK293 cells was examined at 37 °C. The *upper graphs* show the time profiles. *Open* and *closed circles* represent the uptake by Oatp14-transfected cells and vector-transfected cells, respectively. The *lower graphs* show the concentration dependence. Specific uptake was obtained by subtracting the uptake by vector-transfected cells from that by Oatp14-transfected cells. Each *point* represents the mean ± S.E. (n = 3).

saline containing 0.05% Tween 20) and 5% skimmed milk for 1 h at room temperature. After washing with TBS-T, the membrane was incubated with the antibodies (dilution 1:1000). The membrane was allowed to bind a horseradish peroxidase-labeled anti-rabbit IgG antibody (Amersham Biosciences) diluted 1:5000 in TBS-T for 1 h at room temperature followed by washing with TBS-T.

Immunohistochemical Study—Frozen sections from male Sprague-Dawley rats were prepared for the immunohistochemical study after fixing in acetone (−20 °C). The brain slices adhered to the glass cover slips were washed with PBS and fixed for 10 min on ice in acetone. After washing with PBS, the capillaries were permearized in 0.2% (v/v) Triton X-100 in PBS and incubated with peroxidase blocking reagent (DAKO, Carpinteria, CA) for 10 min at room temperature to block nonspecific peroxidase. Slices were incubated with anti-Oatp14 antibody (1:100) for 60 min at room temperature, washed three times with PBS, and subsequently incubated for 60 min at room temperature with the horseradish peroxidase-labeled anti-rabbit secondary antibody (Envision+ system; DAKO). The immune reaction was visualized using diaminobenzidine and then nuclei were stained with hematoxylin (DAKO). The specificity of the antibody reaction was verified by negative controls, which were incubated with polyclonal antibody that had been blocked with the antigenic peptide.

Cloning of Rat Oatp14 cDNA—Based on the nucleotide sequence reported by Li *et al.* (19) (GenBank™ accession number NM 053441), the following primers were designed to isolate Oatp14 cDNA encoding a full open reading frame of Oatp14: forward primer, 5′-ggaattccgccaccatggacacttcatccaaaga-3′ and reverse primer, 5′-ggattccttaaagtcggtctccttgc-3′. PCR was performed using cDNA prepared from rat brain as template according to the following protocol: 96 °C for 1 min, 55 °C for 1 min, and 72 °C for 2 min; 50 cycles. PCR products were subcloned to pGEM-T Easy Vector (Promega, Madison, WI) and sequenced. The nucleotide sequence of rat Oatp14 cDNA was identical as being that of BSAT1 except for one base change (A175G) resulting in a change of amino acid (T59A). However, it was confirmed that this change was not because of an error accumulated during PCR by sequencing the RT-PCR products directly.

Stable Expression of Oatp14 cDNA in HEK293 Cells—The Oatp14-cDNA was subcloned into the pcDNA3.1(+) (Invitrogen) and introduced into HEK293 cells by lipofection with FuGENE 6 (Roche Diagnostics) according to the manufacturer's protocol and were selected by culturing them in the presence of G418 sulfate (800 μg/ml; Invitrogen). HEK293 cells were grown in minimum essential medium (Invitrogen) supplemented with 10% fetal bovine serum, penicillin (100 units/ml), streptomycin (100 μg/ml), and G418 sulfate (400 μg/ml) at 37 °C with 5% CO_2 and 95% humidity. Cells were incubated for 24 h before starting the experiments with culture medium supplemented with sodium butyrate (5 mM).

Transport Study—Uptake was initiated by adding the radiolabeled ligands to the incubating buffer in the presence and absence of inhibitors after cells had been washed three times and preincubated with Krebs-Henseleit buffer (142 mM NaCl, 23.8 mM $NaHCO_3$, 4.83 mM KCl, 0.96 mM KH_2PO_4, 1.20 mM $MgSO_4$, 12.5 mM HEPES, 5 mM glucose, and 1.53 mM $CaCl_2$, adjusted to pH 7.4) at 37 °C for 15 min. For the efflux study, cells were preincubated with [^{125}I]T_4 at 37 °C for 15 min and washed three times with ice-cold Krebs-Henseleit buffer, followed by incubation in the absence of [^{125}I]T_4 with Krebs-Henseleit buffer at 37 °C. The uptake and efflux were terminated at designed times by adding ice-cold Krebs-Henseleit buffer. The radioactivity associated with the cells and medium specimens was determined in a liquid scintillation counter. The remaining aliquots of cell lysates were used to determine protein concentrations by the method of Lowry (23) with bovine serum albumin as a standard. Ligand uptake is given as the cell-to-medium concentration ratio determined as the amount of ligand associated with the cells divided by the medium concentration. Specific uptake was obtained by subtracting the uptake by vector-transfected cells from that by Oatp14-expressed cells.

Kinetic Analyses—Kinetic parameters were obtained from the following Michaelis-Menten equation, $v = V_{max}S/(K_m + S)$, where v is the uptake rate of the substrate (pmol/min/mg protein), S is the substrate concentration in the medium (μM), K_m is the Michaelis-Menten constant (μM), and V_{max} is the maximum uptake rate (pmol/min/mg protein). To obtain the kinetic parameters, the equation was fitted to the initial uptake velocity. The experimental data were fitted to the equation by nonlinear regression analysis with weighting as the reciprocal of the observed values, and the Damping Gauss Newton Method algorithm was used for fitting. Inhibition constants (K_i) for Oatp14-mediated transport were calculated assuming competitive inhibition.

Production of Hyperthyroid and Hypothyroid Conditions—Male Sprague-Dawley rats, weighing 200–220 g, were purchased from Japan SLC (Shizuoka, Japan). Rats had free access to food and water at all times during the study. Production of hyperthyroid and hypothyroid conditions involved a modification of the procedure of Burmeister *et al.* (24). Hypothyroidism was induced by the addition of 0.05% methimazole (MMI), an inhibitor for thyroid hormone synthesis in the thyroid gland, to the drinking water or thyroidectomy. Hypothyroidism was assessed clinically by failure to gain weight at the expected rate and

TABLE I
Substrate specificity of Oatp14

Oatp14-expressed and vector-transfected HEK293 cells were grown to confluence. After 24 h of incubation in culture medium including 5 mM sodium butyrate, uptake was examined in Krebs-Henseleit buffer.

Substrates	Oatp14	pcDNA	Ratio, Oatp14/pcDNA
	μl/mg protein/15 min		
CA	5.66 ± 0.30	5.24 ± 0.43	1.1 ± 0.1
GCA	18.7 ± 2.3	15.7 ± 1.6	1.2 ± 0.2
TCA	8.09 ± 0.52	6.06 ± 0.10	1.3 ± 0.1[a]
LCA	576 ± 6	535 ± 18	1.1 ± 0.0
CDCA	65.7 ± 6.7	84.1 ± 11.5	0.8 ± 0.1
UDCA	10.5 ± 0.1	9.71 ± 0.35	1.1 ± 0.0
TLCS	61.5 ± 1.9	43.7 ± 1.7	1.4 ± 0.1
Estradiol	204 ± 4	186 ± 13	1.1 ± 0.1
Testosterone	52.3 ± 1.5	39.2 ± 1.4	1.3 ± 0.1[b]
Dihydrotestosterone	147 ± 15	106 ± 5	1.4 ± 0.2[b]
Corticosterone	24.7 ± 1.5	20.9 ± 0.5	1.2 ± 0.1
Estrone	303 ± 15	248 ± 6	1.2 ± 0.1[a]
DHEAS	9.68 ± 0.24	7.72 ± 0.48	1.3 ± 0.1[a]
Estrone-sulfate	11.1 ± 0.8	6.3 ± 0.1	1.7 ± 0.1[a]
$E_2$17βG	50.1 ± 4.7	2.4 ± 0.2	21.2 ± 2.9[b]
LTC4	14.5 ± 0.6	13.4 ± 0.1	1.1 ± 0.0[b]
LTD4	19.6 ± 0.8	18.0 ± 2.0	1.1 ± 0.1
LTE4	30.5 ± 1.3	26.0 ± 0.9	1.2 ± 0.1[a]
PGD2	3.50 ± 0.15	3.61 ± 0.12	1.0 ± 0.1
PGE2	6.99 ± 0.46	5.80 ± 0.24	1.2 ± 0.1
Leu-Enkephalin	54.2 ± 2.9	43.3 ± 2.5	1.3 ± 0.1[a]
CCK-8	2.58 ± 0.21	1.81 ± 0.13	1.4 ± 0.2[a]
T3	951 ± 16	733 ± 4	1.3 ± 0.0[b]
Reverse T3	1397 ± 79	71 ± 5	19.7 ± 1.7[b]
T4	1456 ± 10	124 ± 3	11.8 ± 0.3[b]
Ketoprofen	9.53 ± 0.42	6.91 ± 0.26	1.4 ± 0.1[b]
Ibuprofen	3.18 ± 0.11	3.99 ± 1.18	0.8 ± 0.2
Indomethacin	31.3 ± 0.9	34.3 ± 2.0	0.9 ± 0.1
Benzylpenicillin	5.76 ± 0.47	5.45 ± 0.12	1.1 ± 0.1
OchratoxinA	8.58 ± 1.29	5.81 ± 0.14	1.5 ± 0.2[b]
Qunidine	1390 ± 34	1274 ± 150	1.1 ± 0.1
Cerivastatin	105 ± 2	33 ± 1	3.1 ± 0.1[b]
Pravastatin	5.62 ± 0.38	3.50 ± 0.75	1.6 ± 0.4[a]
Digoxin	8.70 ± 0.13	9.96 ± 0.22	0.9 ± 0.0
E3040	106 ± 3	93 ± 5	1.1 ± 0.1
E3040G	10.7 ± 1.0	2.12 ± 0.22	5.1 ± 0.7[a]
E3040S	4.78 ± 0.35	1.69 ± 0.26	2.8 ± 0.5[b]
4MUS	1.82 ± 0.35	0.90 ± 0.03	2.0 ± 0.1[b]
Troglitazone-sulfate	64.1 ± 14.3	8.4 ± 0.4	7.6 ± 1.7[b]

[a] Statistically significant uptake is indicated. $p < 0.05$.
[b] Statistically significant uptake is indicated. $p < 0.01$.

TABLE II
K_m, V_{max} and V_{max}/K_m values for Oatp14

The K_m and V_{max} values were determined by nonlinear regression analysis using data shown in Fig. 3.

Substrate	K_m	V_{max}	V_{max}/K_m
	μM	*pmol/min/mg protein*	*μl/min/mg protein*
$E_2$17βG	10.7 ± 1.6	93.4 ± 10.4	8.73 ± 1.63
Cerivastatin	1.34 ± 0.25	14.5 ± 2.2	10.8 ± 2.6
TRO-S	0.76 ± 0.09	69.0 ± 6.7	91.3 ± 14.2
T4	0.18 ± 0.03	32.1 ± 2.5	147 ± 14

could be observed within 2 weeks of the beginning MMI treatment and within 1 week after thyroidectomy. Hyperthyrodism was produced by giving L-T3 (50 μg/100 g body weight, subcutaneously, daily) 4 days before capillary isolation.

RESULTS

Tissue Distribution of Oatp14—The expression of Oatp14 mRNA in rat tissues was investigated by Northern blot analysis (Fig. 1*A*). A band was detected at 2.6 kbp, predominantly in the brain. No hybridization signals were detected in mRNA isolated from other tissues, including the heart, spleen, lung, liver, skeletal muscle, kidney, and testis.

Immunoblot and Immunohistochemical Staining of Oatp14—The expression of Oatp14 in the choroid plexus, brain homogenate, and brain capillary was examined by Western blot analysis (Fig. 1*B*). Immunoreactive protein was detected at ~90 kDa in the choroid plexus, brain homogenate, and brain capillary. These bands were abolished when preabsorbed polyclonal antibody for Oatp14 was used, suggesting that the positive bands were specific for the antigen peptide.

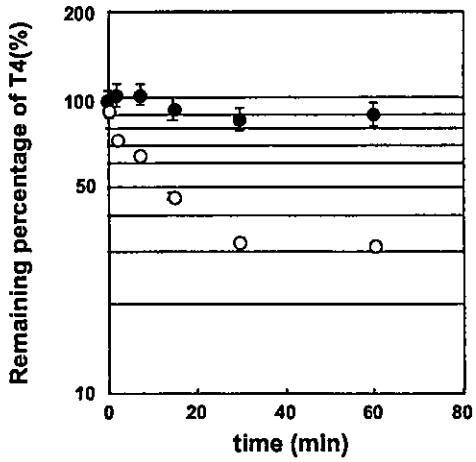

FIG. 4. **Time profiles of the efflux of [^{125}I]T_4 from Oatp14-transfected HEK293 cells.** The efflux of preloaded [^{125}I]T_4 from Oatp14-transfected HEK293 cells was examined at 37 °C. *Open* and *closed circles* represent the efflux from Oatp14- and vector-transfected cells, respectively. Each *point* represents the mean ± S.E. (n = 3).

To investigate the localization of Oatp14 in brain capillary endothelial cells, immunohistochemical staining was carried out using anti-Oatp14 polyclonal antibody (Fig. 2). Positive signals for anti-Oatp14 polyclonal antibody were detected in brain capillary endothelial cells. The signals were detected along the plasma membrane of brain capillary endothelial cells. The signal was abolished by preincubating the polyclonal antibody of Oatp14 with antigen (data not shown).

Transport Properties of Oatp14—Fig. 3 shows the time profiles of the uptake of [^{3}H]$E_2$17βG (*A*), [^{14}C]cerivastatin (*B*), [^{35}S]TRO-S (*C*), and [^{125}I]T_4 (*D*) by Oatp14-expressed HEK293 cells and vector-transfected HEK293 cells. Their uptake by Oatp14-expressed cells is markedly greater than that by vector-transfected cells. This Oatp14-mediated uptake showed saturation kinetics and followed the Michaelis-Menten equation (Fig. 3, *E-H*). The kinetic parameters for the uptake by Oatp14 were determined by nonlinear regression analysis and summarized in Table I. The uptake of various organic anions by Oatp14 was investigated, and the results are summarized in Table II. The uptake of [^{14}C]E3040 glucuronide, [^{14}C]E3040 sulfate, [^{14}C]4-MUS, and [^{125}I]reverse T_3 by Oatp14-expressed cells was significantly greater compared with that by vector-transfected (Table II). Although the triiodothyronine (T_3) uptake by Oatp14-expressed cells was significantly greater than that by vector-transfected cells, the Oatp14-mediated uptake for T_3 was ~6-fold smaller than that of T_4 and reverse T_3 by Oatp14 (Table II). The difference in the uptake of [^{3}H]taurocholate, [^{3}H]TLCS, [^{3}H]testosterone, [^{3}H]dihydrotestosterone, [^{3}H]estrone, [^{3}H]estrone sulfate (ES), [^{3}H]dehydroepiandrosterone sulfate, [^{3}H]leukotriene E_4 (LTE_4), [^{3}H]Leu-enkephalin, [^{3}H]cholecystokinin-octapeptide (CCK-8), [^{125}I]T_3, [^{3}H]pravastatin, [^{3}H]ketoprofen, and [^{3}H]ochratoxin A was statistically significant between Oatp14-expressed and vector-transfected cells, although the rates of uptake were very low (Table II).

To investigate whether Oatp14 can mediate bidirectional transport, cells were preloaded with [^{125}I]T_4 for 15 min followed by incubation in the absence of [^{125}I]T_4. The radioactivity associated with cell specimens was rapidly reduced in Oatp14-expressed HEK293 cells compared with that in vector-trans-

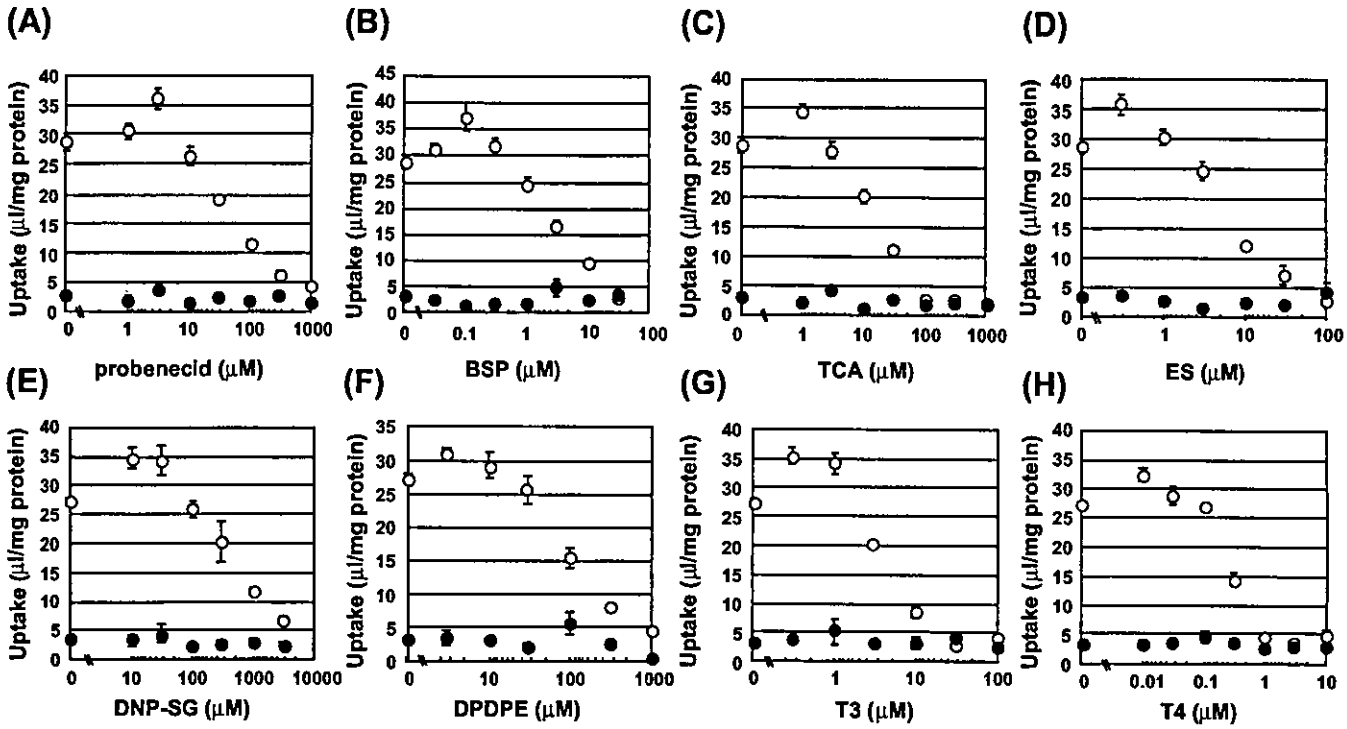

FIG. 5. **Effects of unlabeled probenecid, BSP, trichloroacetic acid, ES, DNP-SG, DPDPE, T_3, and T_4 on the uptake of [^{3}H]$E_2$17βG by Oatp14-transfected HEK293 cells.** The effects of unlabeled probenecid (*A*), BSP (*B*), taurocholate (*TCA*; *C*), ES (*D*), DNP-SG (*E*), DPDPE (*F*), T_3 (*G*), and T_4 (*H*) on the uptake of [^{3}H]$E_2$17βG by Oatp14-transfected HEK293 cells were examined at 37 °C. The specific uptake was obtained by subtracting the uptake by vector-transfected cells from that by gene-transfected cells. *Open* and *closed circles* represent the uptake by Oatp14- and vector-transfected cells, respectively. Each *point* represents the mean ± S.E. (n = 3).

fected cells, and the elimination rate constants were 0.032 ± 0.002 and 0.006 ± 0.001 min^{-1}, respectively (Fig. 4).

cis-inhibitory effects on the Oatp14-mediated uptake of [^{3}H]$E_2$17βG were investigated (Fig. 5). Sulfobromophthalein (BSP), pravastatin, ES, and trichloroacetic acid were potent inhibitors of Oatp14, whereas probenecid was a moderate inhibitor (Fig. 5). *p*-Aminohippurate and cimetidine, typical substrates of organic anion and cation transporters, had no effect on the Oatp14-mediated uptake, whereas benzylpenicillin was a weak inhibitor (Fig. 6). Leukotriene C_4 (*LTC_4*) and glutathione (*GSH*) had no effect, but dinitrophenyl-s-glutathione (*DNP-SG*) was a weak inhibitor (see Figs. 5 and 6). No inhibitory effect by folates (methotrexate, folate, and 5-methyltetrahydrofolate) or tetraethylammonium was observed (Fig. 6). The K_i values of probenecid, BSP, trichloroacetic acid, ES, DNP-SG, DPDPE, T_3, and T_4 for the uptake of [^{3}H]$E_2$17βG by Oatp14-expressed HEK cells are summarized in Table III.

Effects of Hyperthyroid and Hypothyroid Conditions on the Expression of Oatp14 in the Brain Capillary—The effects of hyper- and hypothyroid conditions on the expression of Oatp14 in the brain capillary were investigated by RT-PCR and Western blotting (Fig. 7, *A* and *B*). RT-PCR and Western blotting analyses revealed that the expression levels of Oatp14 mRNA and protein were up- and down-regulated under hypothyroid and hyperthyroid conditions, respectively.

DISCUSSION

In the present study, we reported the substrate specificity of Oatp14, as well as its tissue distribution and localization in the brain. Oatp14 is expressed in the brain capillary and choroid plexus. It mediated the uptake of T_3, T_4, and reverse T_3, as well as organic anions such as $E_2$17βG, cerivastatin, and TRO-S, suggesting its involvement in the membrane transport of these ligands in the brain capillary.

T_3 and its prohormone, T_4, are produced in the thyroid gland and released into the blood. T_3 plays an essential role in brain development via binding to specific nuclear receptors (thyroid hormone receptor) (25). Deficiency of thyroid hormones particularly during fetal and neonatal period in the brain causes mental retardation and cretinism (26, 27). T_3 is supplied to the brain and peripheral tissues as T_4 from which T_3 is enzymatically produced by type 2 iodothyronine deiodinase (D2) (25). Therefore, the brain uptake process of T_4 from the circulating blood is the first step in all subsequent reactions of thyroid hormone in the brain. Whether there is a specific transport mechanism(s) for T_4 in brain capillary endothelial cells remains controversial. The brain uptake of T_4 was saturable in dogs (28) but not in mice (29). Analysis of the transport and molecular properties of Oatp14 should help us resolve this.

Transfection of Oatp14 cDNA into HEK293 cells resulted in a marked increase in the uptake of T_4, as well as reverse T_3, an inactive metabolite of T_4 produced by type 3 iodothyronine deiodinase. Although the uptake of T_3 by Oatp14-expressed cells was significantly greater than that by vector-transfected cells (Table II), T_3 was extensively taken up by vector-transfected cells (Table II). Whether the uptake in vector-transfected cells is ascribed to specific transport system(s) for T_3 or passive diffusion remains unknown. The transport activity for T_3 exhibited by Oatp14, obtained by subtraction of the uptake by vector-transfected cells from that by Oatp14-expressed cells, was ~6-fold lower than that for T_4 and reverse T_3 by Oatp14 (Table II), although the chemical structures of T_3 and reverse T_3 are quite similar. The K_i value of T_3 for Oatp14 was 25-fold greater than that of T_4 (Table III), and this may result in apparent low transport activity for T_3 by Oatp14. Oatp14 can also mediate bidirectional transport, because the efflux of T_4 is facilitated in Oatp14-expressed cells (Fig. 4), and it is possible that Oatp14 is involved in both the uptake and efflux of its ligands through the brain capillary (*i.e.* BBB).

Involvement of Oatp14 in maintaining homeostasis of T_4 in the brain was also supported by the change in expression levels

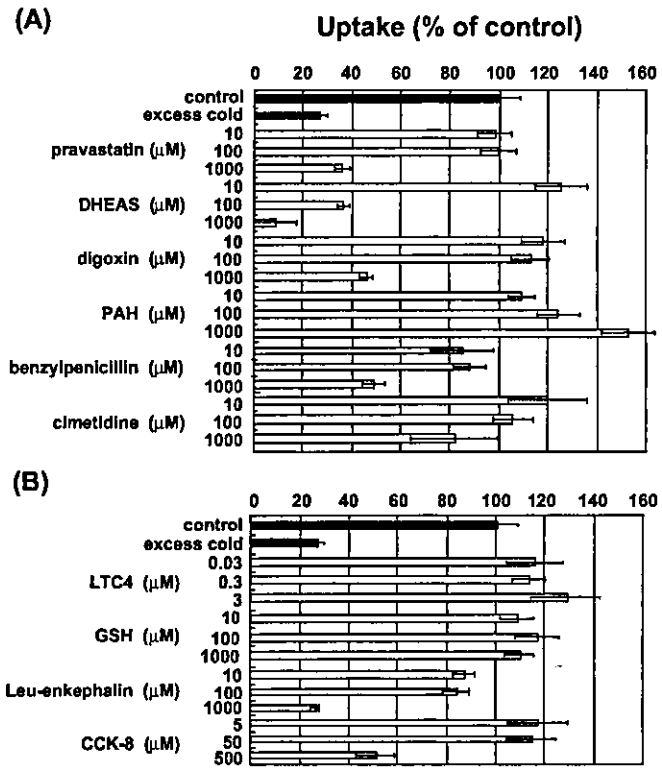

FIG. 6. **Effects of several unlabeled compounds on the uptake of [^{3}H]$E_2$17βG by Oatp14-transfected HEK293 cells.** The effects of several unlabeled compounds on the uptake of [^{3}H]$E_2$17βG by Oatp14-transfected HEK293 cells were examined at 37 °C. Results are given as a ratio with respect to the control values determined in the absence of unlabeled compounds. Each *point* represents the mean ± S.E. (n = 3). *DHEAS*, dehydroepiandrosterone sulfate; *PAH*, *p*-aminohippurate; *GSH*, glutathione; *CCK-8*, cholecystokinin-octapeptide.

TABLE III
K_i values for Oatp14

The K_i values were determined by nonlinear regression analysis using data shown in Fig. 5.

Inhibitor	K_i
	μM
Probenecid	39.5 ± 8.3
BSP	4.18 ± 1.02
Taurocholate	7.24 ± 3.33
ES	6.63 ± 1.62
DNP-SG	467 ± 67
DPDPE	86.3 ± 11.2
T3	2.46 ± 0.96
T4	0.11 ± 0.04

of Oatp14 in the brain capillary under hypo- and hyperthyroid conditions (Fig. 7). The expression of Oatp14 in the brain capillary changed as if Oatp14 was responsible for maintaining the concentration of T_4 in the central nervous system: up- and down-regulated under hypothyroid and hyperthyroid conditions, respectively (Fig. 7). This pattern is similar to that observed in D2 expression (25). Increased D2 expression increases the conversion of T_4 to T_3 to compensate for the decrease in the local brain concentration of T_4 and vice versa. Therefore, we hypothesize that Oatp14 is involved in the uptake of T_4 through the brain capillaries.

In addition to Oatp14, Oatp2, the other isoform of rat Oatp family, is also the candidate transporter for T_3 and T_4 uptake by the brain from the circulating blood in rodents. The uptake of both T_3 and T_4 was significantly increased in Oatp2-cRNA injected oocytes with similar K_m values (~5–7 μM) (12). Oatp2 has been identified both in the luminal and abluminal membrane of brain capillary endothelial cells (15). It is possible that Oatp14 and Oatp2 serve high and low affinity sites for T_4 in the brain capillary, because the K_m values of Oatp2 were ~30-fold greater than that of Oatp14 (12). Following uptake from the circulating blood into endothelial cells, T_4 has to cross the abluminal membrane to reach the brain interstitial space and brain parenchymal cells. Whether this process is carrier-mediated remains unknown. Bidirectional nature of Oatp2-mediated transport has been reported in Oatp2-cRNA-injected oocytes (30). Oatp14 and Oatp2 are candidate transporters involved in the abluminal secretion of thyroid hormones. Further studies are necessary to identify the exact localization of Oatp14 in the brain capillary and to evaluate its contribution to the total brain uptake of T_4 into the brain. Pardridge *et al.* (31) demonstrated that the brain uptake of T_3 was saturable and inhibited by T_4 using carotid arterial bolus injection technique of Oldendorf, and Oatp2 may account for the brain uptake of T_3 in the brain capillary.

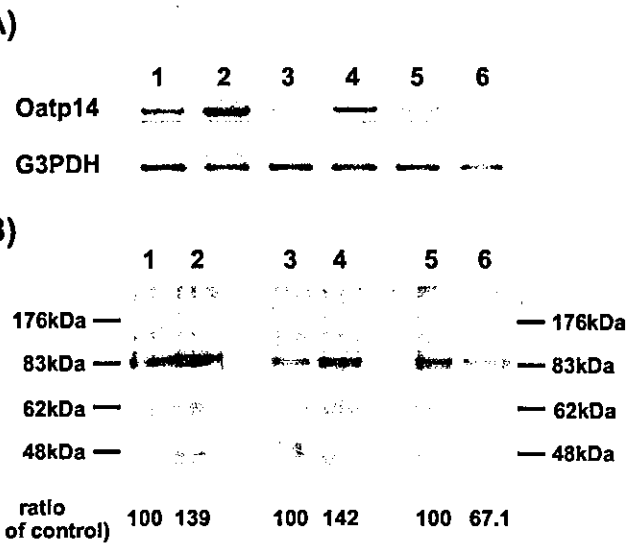

FIG. 7. **Effect of hyperthyroid and hypothyroid conditions on the expression of Oatp14 on the BBB.** *A*, RT-PCR analysis. mRNA samples were prepared from isolated brain capillary from control rats (*lanes 1, 3,* and *5*), hypothyroid rats (MMI-treated or thyroidectomized rats; *lanes 2* and *4*, respectively) and hyperthyroid rats (T_3-treated rats; *lane 6*). PCR products stained with ethidium bromide were visualized under UV light. *G3PDH*, glucose-3-phosphate dehydrogenase. *B*, Western blotting. Brain capillaries (50 μg/*lane*) isolated from control rats (*lanes 1, 3,* and *5*), hypothyroid rats (MMI-treated or thyroidectomized rats; *lanes 2* and *4*, respectively), and hyperthyroid rats (T_3-treated rats; *lane 6*) were separated by SDS-PAGE (10% separating gel). Oatp14 was detected by anti-Oatp14 polyclonal antibody.

Oatp14 was detected in the choroid plexus by Western blot analysis (Fig. 1). The choroid plexus is located in the lateral, third and fourth ventricles, and the interface between the cerebrospinal fluid and the circulating blood acting as a barrier to protect the central nervous system, in conjunction with the BBB (32, 33). The brain distribution of T_3 and T_4 after intracerebroventricular administration is limited to ependymal cells and circumventricular organs and, thus, transport via the choroid plexus could account for the brain distribution near the ventricles (34). As speculated in the case of brain capillary endothelial cells, it is possible that Oatp14 acts as an uptake system to supply T_4 to ependymal cells and circumventricular organs in the choroid plexus.

In addition to thyroids, Oatp14 accepts certain types of amphipathic organic anions, such as $E_2$17βG, cerivastatin, and TRO-S, as substrates although their transport activity was markedly lower than that of T_4, except TRO-S (see Fig. 3 and Table II). Because Oatp14 can mediate the bidirectional trans-

port, it is possible that Oatp14 is involved in the efflux of organic anions such as $E_2 17\beta G$ from the brain when it is microinjected into the cerebral cortex and possibly in the efflux of excess T_4 and reverse T_3 from the brain. The spectrum of inhibitors of Oatp14 was consistent with the transporter hypothesized based on *in vivo* studies (18), but further investigations will be required to confirm this speculation.

Whether the results obtained using cDNA from rodents can be applied to the human situation is an important issue. Human OATP-F, an isoform in which Oatp14 exhibits high homology (84% in amino acid level), has a similar substrate specificity to Oatp14 (35). Northern blot analysis demonstrated abundant expression of OATP-F in the brain and testis and, to a lesser extent, heart, but the localization in the brain remains unidentified. In terms of substrate specificity and homology, OATP-F is supposed to be the human ortholog of Oatp14, and it may be suggested that OATP-F is also involved in the uptake of T_4 from the circulating blood into the central nervous system though the brain capillary and choroid plexus. In view of the importance of supplying T_4 to the brain during development, it is possible that functional loss of the OATP-F gene may be associated with a thyroid hormone-related neuronal disorder characterized by resistance to thyroid hormone treatment.

In conclusion, we have characterized Oatp14 in terms of its substrate specificity and localization in the brain and demonstrated that Oatp14 accepts T_4, as well as organic anions, including certain glucuronide and sulfate conjugates. Oatp14 is localized on the plasma membrane of brain capillary endothelial cells and involved in the uptake of T_4 from the blood to the central nervous system. Oatp14 is one of the mechanisms for maintaining homeostasis of T_4 and, ultimately, T_3 in the brain.

REFERENCES

1. Rapoport, S. I. (1976) *Exp. Neurol.* **52,** 467–479
2. Pardridge, W. M. (1991) *Semin. Cell Biol.* **2,** 419–426
3. Minn, A., Ghersi-Egea, J. F., Perrin, R., Leininger, B., and Siest, G. (1991) *Brain Res. Brain Res. Rev.* **16,** 65–82
4. Strazielle, N., and Ghersi-Egea, J. F. (1999) *J. Neurosci.* **15,** 6275–6289
5. Suzuki, H., Terasaki, T., and Sugiyama, Y. (1997) *Adv. Drug. Deliv. Rev.* **25,** 257–285
6. Kusuhara, H., and Sugiyama, Y. (2001) *Drug Discov. Today* **6,** 150–156
7. Lee, G., Dallas, M., Hong, M., and Bendayan, R. (2001) *Pharmacol. Rev.* **52,** 569–596
8. Kullak-Ublick, G. A., Stieger, B., Hagenbuch, B., and Meier, P. J. (2000) *Semin. Liver Dis.* **20,** 273–292
9. Kullak-Ublick, G. A., Ismair, M. G., Stieger, B., Landmann, L., Huber, R., Pizzagalli, F., Fattinger, K., Meier, P. J., and Hagenbuch. B. (2001) *Gastroenterology* **120,** 525–533
10. Jacquemin, E., Hagenbuch, B., Stieger, B., Wolkoff, A. W., and Meier, P. J. (1994) *Proc. Natl. Acad. Sci. U.S.A.* **91,** 133–137
11. Noe, B., Hagenbuch, B., Stieger, B., and Meier, P. J. (1997) *Proc. Natl. Acad. Sci. U. S. A.* **94,** 10346–11035
12. Abe, T., Kakyo, M., Sakagami, H., Tokui, T., Nishio, T., Tanemoto, M., Nomura, H., Hebert, S. C., Matsuno, S., Kondo, H., and Yawo, H. (1998) *J. Biol. Chem.* **273,** 22395–22401
13. Nishio, T., Adachi, H., Nakagomi, R., Tokui, T., Sato, E., Tanamoto, M., Fujiwara, K., Okabe, M., Onogawa, T., Suzuki, T., Nakai, D., Shiiba, K., Suzuki, M., Ohtani, H., Kondo, Y., Unno, M., Ito, S., Iinuma, K., Nunoki, K., Matsuno, S., and Abe, T. (2000) *Biochem. Biophys. Res. Commun.* **275,** 831–838
14. Kullak-Ublick, G. A., Hagenbuch, B., Stieger, B., Schteingart, C. D., Hofmann, A. F., Wolkoff, A. W., and Meier, P. J. (1995) *Gastroenterology* **109,** 1274–1282
15. Gao, B., Stieger, B., Noe, B., Fritschy, J. M., and Meier, P. J. (1999) *J. Histochem. Cytochem.* **47,** 1255–1264
16. Gao, B., Hagenbuch, B., Kullak-Ublick, G. A., Benke, D., Aguzzi, A., and Meier, P. J. (2000) *J. Pharmacol. Exp. Ther.* **294,** 73–79
17. Dagenais, C., Ducharme, J., and Pollack, G. M. (2001) *Neurosci. Lett.* **301,** 155–158
18. Sugiyama, D., Kusuhara, H., Shitara, Y., Abe, T., Meier, P. J., Sekine, T., Endou, H., Suzuki, H., and Sugiyama, Y. (2001) *J. Pharmacol. Exp. Ther.* **298,** 316–322
19. Li, J. Y., Boado, R., and Pardridge, W. M. (2001) *J. Cereb. Blood Flow Metab.* **21,** 61–68
20. Izumi, T., Hosiyama, K., Enomoto, S., Sasahara, K., and Sugiyama, Y. (1997) *J. Pharmacol. Exp. Ther.* **280,** 1392–40021
21. Akita, H., Suzuki, H., Ito, K., Kinoshita, S., Sato, N., Takikawa, H., and Sugiyama, Y. (2001) *Biochim. Biophys. Acta* **1511,** 7–16
22. Boado, R. J., and Pardridge, W. M. (1991) *J. Neurochem.* **57,** 2136–2139
23. Lowry, O. (1951) *J. Biol. Chem.* **193,** 265–273
24. Burmeister, L. A., Pachucki, J., and Germain, D. L. S. (1997) *Endocrinology* **138,** 5231–5237
25. Forrest, D., Reh, T. A., and Rusch, A. (2002) *Curr. Opin. Neurol.* **12,** 49–56
26. Oppenheimer, J. H., and Schwartz, H. L. (1997) *Endocr. Rev.* **18,** 462–475
27. Shi, Y. B., Ritchie, J. W. A., and Taylor, P. M. (2002) *Pharmacol. Ther.* **94,** 235–251
28. Hagen, G. A., and Solberg, L. A., Jr. (1974) *Endocrinology* **95,** 1398–1410
29. Banks, W. A., Kastin, A. J., and Micahls, E. A. (1985) *Life Sci.* **37,** 2407–2414
30. Li, L., Meier, P. J., and Ballatori, N. (2000) *Mol. Pharmacol.* **58,** 335–340
31. Pardridge, W. M. (1979) *Endocrinology* **105,** 605–612
32. Groothuis, D. R., and Levy, R. M. (1997) *J. Neurovirol.* **3,** 387–400
33. Segal, M. B. (2000) *Cell. Mol. Neurobiol.* **20,** 183–196
34. Dratman, M. B., Chrutchfield, F. L., and Schoenhoff, M. B. (1991) *Brain Res.* **554,** 229–236
35. Pizzagalli, F., Hagenbuch, B., Stieger, B., Klenk, U., Folkers, G., and Meier, P. J. (2002) *Mol. Endocrinol.* **16,** 2283–2296

0031-6997/03/5503-425–461$7.00
PHARMACOLOGICAL REVIEWS
Vol. 55, No. 3
30301/1082282
Printed in U.S.A

Pharmacol Rev 55:425–461, 2003

Impact of Drug Transporter Studies on Drug Discovery and Development

NAOMI MIZUNO, TAKURO NIWA, YOSHIHISA YOTSUMOTO, AND YUICHI SUGIYAMA

Graduate School of Pharmaceutical Sciences, University of Tokyo, Tokyo, Japan; and Pharmacokinetics Laboratory, Mitsubishi Pharma Corporation, Chiba, Japan

***Abstract*—Drug transporters are expressed in many tissues such as the intestine, liver, kidney, and brain, and play key roles in drug absorption, distribution, and excretion. The information on the functional characteristics of drug transporters provides important information to allow improvements in drug delivery or drug design by targeting specific transporter proteins. In this article we summarize the significant role played by drug transporters in drug disposition, focusing particularly on their potential use during the drug discovery and development process. The use of transporter function offers the possibility of delivering a drug to the target organ, avoiding distribution to other organs (thereby reducing the chance of toxic side effects), controlling the elimination process, and/or improving oral bioavailability. It is useful to select a lead compound that may or may not interact with transporters, depending on whether such an interaction is desirable. The expression system of transporters is an efficient tool for screening the activity of individual transport processes. The changes in pharmacokinetics due to genetic polymorphisms and drug-**

Address correspondence to: Dr. Yuichi Sugiyama, Graduate School of Pharmaceutical Sciences, The University of Tokyo, 7-3-1 Hongo, Bunkyo-ku, Tokyo 113-0033, Japan. E-mail: sugiyama@mol.f.u-tokyo.ac.jp

Article, publication date, and citation information can be found at http://pharmrev.aspetjournals.org.
DOI: 10.1124/pr.55.3.1.

drug interactions involving transporters can often have a direct and adverse effect on the therapeutic safety and efficacy of many important drugs. To obtain detailed information about these interindividual differences, the contribution made by transporters to drug absorption, distribution, and excretion needs to be taken into account throughout the drug discovery and development process.

I. Introduction

With publication of the complete human genome sequence in 2001 (International Human Genome Sequencing Consortium, 2001; Venter et al., 2001), this new information about all the human genes and their functions led to a change in drug research strategies and, in particular, the processes of drug discovery and development. Following the progress in genome-based drug discovery, international competition in drug discovery has become even keener. The particular strategy adopted for drug discovery will be a critical factor in determining whether a company is successful in its research and development operations. The strategy that target proteins are identified based on genomic information, so-called "genome-based drug discovery," is likely to become very popular. However, determination of the target protein alone is insufficient to allow the development of clinically significant drugs. It is also necessary to identify the lead compounds binding the target proteins by using combinatorial chemistry synthesis and high-throughput screening, optimize these lead compounds, and then select those with clinically effective pharmacological activity and minimize any side effects. A significant number of drug candidates entering clinical development are dropped at some stage due to unacceptable pharmacokinetic properties (White, 2000; Roberts, 2001). The pharmacokinetic profile should be a primary consideration in the selection of a drug candidate, ultimately contributing to its eventual clinical success or failure. It is now recognized that selection of a "robust" candidate requires a balance among efficacy, safety, and pharmacokinetic properties, and that the screening of these characteristics should be carried out as early as possible in the discovery process. Thus, many pharmaceutical companies are now carrying out rational high-throughput drug metabolism and pharmacokinetics screening systematically and establishing pharmacokinetic selection criteria (White, 2000; Roberts, 2001). For example, the high-throughput screening for absorption using Caco-2 cells and the screening for metabolic stability and metabolic enzyme inhibition using cytochrome P450 recombinant microsomes or human liver microsomes have become extremely popular. Attention is now being focused on optimizing the pharmacokinetic profiles of drug candidates using transporter function (Ayrton and Morgan, 2001; Mizuno and Sugiyama, 2002).

Many different drug transporters are expressed in various tissues, such as the epithelial cells of the intestine and kidney, hepatocytes, and brain capillary endothelial cells (Muller and Jansen, 1997; Koepsell, 1998; Meijer et al., 1999; Suzuki and Sugiyama, 1999; Inui et al., 2000a; van Aubel et al., 2000; Gao and Meier, 2001) (Table 1). In recent years, a number of important transporters have been cloned, and considerable progress has been made in understanding the molecular characteristics of individual transporters. It has now become clear that some of these are responsible for drug transport in various tissues, and they may be key determinants of the pharmacokinetic characteristics of a drug as far as its intestinal absorption, tissue distribution, and elimination are concerned (Oude Elferink et al., 1995; Zhang et al., 1998; Kim, 2000; Dresser et al., 2001; Kusuhara and Sugiyama, 2002; Russel et al., 2002). Studies of the functional characteristics, such as substrate specificity, and of the localization of cloned drug transporters could provide important information about the mechanisms of drug disposition. Transporters have been classified as primary, secondary, or tertiary active transporters. Secondary or tertiary active transporters, such as OAT[1], OATP, NTCP, OCT, OCTN, and PEPT, are driven by an exchange or cotransport of intracellular and/or extracellular ions (Burckhardt and Wolff, 2000; Dresser et al., 2001; Lee et al., 2001a). The driving force for primary active transporters like ATP-binding cassette transporters, such as MDR, MRP, and BCRP, is ATP hydrolysis

[1]Abbreviations: OAT, organic anion transporter; OATP, organic anion-transporting polypeptide; NTCP, sodium taurocholate cotransporting peptide; OCT, organic cation transporter; PEPT, oligopeptide transporter; ASBT, apical sodium-dependent bile acid transporter; MDR, multidrug resistant (or resistance); MRP, multidrug resistance-associated protein; BCRP, breast cancer resistance protein; SLC, solute carrier superfamily; ABC, ATP-binding cassette; BBB, blood-brain barrier; CNS, central nervous system; P-gp, P-glycoprotein; ACE, angiotensin-converting enzyme; AUC, area under concentration-time curve; TPGS, *d*-α-tocopheryl polyethylene glycol 1000 succinate; HIV, human immunodeficiency virus; PS, permeability-surface area; CL, clearance; E_2-17βG, estradiol-17β-glucuronide; PAH, *p*-aminohippurate; NSAID(s), nonsteroidal anti-inflammatory drug(s); CPT-11, irinotecan hydrochloride; CMV, canalicular membrane vesicle; BSEP, bile salt export pump; $CL_{int,bile}$, intrinsic clearance for the net biliary excretion from the blood; PS_1, hepatic uptake across the sinusoidal membrane; PS_2, efflux across the sinusoidal membrane from the liver; PS_3, excretion across the canalicular membrane; HIV-PI, HIV protease inhibitor; SXR, steroid xenobiotic receptor; PXR, pregnane X receptor; GS-X, glutathione *S*-conjugate export; FXR, farnesoid X-activated receptor; CAR, constitutive androstane receptor; HNF1, hepatocyte nuclear factor 1; CFTR, cystic fibrosis transmembrane conductance regulator; DJS, Dubin-Johnson syndrome; ER, endoplasmic reticulum; *Rdx*, radixin; SNP, single nucleotide polymorphism; K_p, tissue-to-plasma concentration ratio; LC/MS/MS, liquid chromatography/tandem mass spectrometry; P_{app}, apparent permeability; TCA, taurocholate; AM, acetoxymethyl ester.

allowing the rational prediction and extrapolation of in vivo drug disposition from in vitro data are urgently required. Although there has been intensive investigation of the functional analysis of the human genome, there are a large number of genes whose molecular protein function remains unknown (Venter et al., 2001). The human genome contains many genes that encode membrane transporters and related proteins (Table 3) (Venter et al., 2001). For drug discovery, development, and targeting one needs to know which transporters play a role in the disposition of a drug and its subsequent effects.

In this article, we summarize the key role played by drug transporters in drug disposition, and the strategic use of drug transporters in drug discovery and development is discussed. We also introduce possible strategies for drug discovery using transporters, including the transporter screening systems, methods for estimating the contribution of transporters to drug disposition, and the prediction of in vivo drug disposition from in vitro data.

II. Strategies for Drug Discovery Using Transporters

A. Drug Delivery to Target Tissues Using Transporters

One of the main goals is to develop pharmaceutical agents with no adverse effects. It is also desirable to develop drugs with a wide therapeutic spectrum of activity. Drug targeting is one effective approach both to increase the pharmacological activity of drugs and to reduce their side effects by enhancing delivery to the target site. Recent research has identified many types of transporters that are expressed selectively in the liver, kidney, and other organs and which, therefore, may be a promising target for drug delivery. Some instances of drug delivery to the liver or kidney are introduced here.

The most comprehensively documented case is pravastatin. Pravastatin, a 3-hydroxy-3-methylglutaryl-coenzyme A reductase inhibitor, undergoes enterohepatic circulation, which prolongs the exposures of the liver (target organ) to the drug and minimizes adverse side effects in the peripheral tissues. This enterohepatic circulation is mediated by transporters in every process from pravastatin gastrointestinal absorption to biliary transport. Pravastatin is taken up by the liver from the portal vein by OATP family proteins located on the sinusoidal (basolateral) membrane (Hsiang et al., 1999; Nakai et al., 2001; Sasaki et al., 2002). After exhibiting its pharmacological action in the liver, pravastatin is then excreted into the bile via MRP2 with only a minimum degree of metabolic conversion (Yamazaki et al., 1996). The fraction of the drug released into the duodenum is then reabsorbed by active transport (Tamai et al., 1995). Thus, efficient hepatobiliary transport by OATP and MRP2 plays an important role in the enterohepatic circulation, which is responsible for maintaining significant concentrations of this drug in the liver. Although the mechanisms governing the pharmacokinetic properties of this drug were identified after their development, attempts to design molecules during the drug discovery process will be required in the future.

It has been found that successful targeting of anticancer drugs can be achieved using oligopeptide transporter

TABLE 2
Abbreviations of human drug transporters

Abbreviation		Symbol[a]
MDR1/P-gp	Multidrug resistant gene/P-glycoprotein	*ABCB1*
BSEP/SPGP	Bile salt export pump/sister P-glycoprotein	*ABCB11*
MRP1	Multidrug resistance associated protein 1	*ABCC1*
MRP2/cMOAT	Multidrug resistance associated protein 2	*ABCC2*
MRP3	Multidrug resistance associated protein 3	*ABCC3*
MRP4	Multidrug resistance associated protein 4	*ABCC4*
BCRP	Breast cancer resistance protein	*ABCG2*
NTCP	Sodium taurocholate cotransporting peptide	*SLC10A1*
ASBT	Apical sodium-dependent bile acid transporter	*SLC10A2*
PEPT1	Oligopeptide transporter 1	*SLC15A1*
PEPT2	Oligopeptide transporter 2	*SLC15A2*
OATP-A	Organic anion transporting polypeptide-A	*SLC21A3*
OATP-C/OATP2/LST-1	Organic anion transporting polypeptide-C	*SLC21A6*
OATP8	Organic anion transporting polypeptide 8	*SLC21A8*
OATP-B	Organic anion transporting polypeptide-B	*SLC21A9*
OATP-D	Organic anion transporting polypeptide-D	*SLC21A11*
OATP-E	Organic anion transporting polypeptide-E	*SLC21A12*
OATP-F	Organic anion transporting polypeptide-F	*SLC21A14*
OCT1	Organic cation transporter 1	*SLC22A1*
OCT2	Organic cation transporter 2	*SLC22A2*
OCT3	Organic cation transporter 3	*SLC22A3*
OCTN1	Novel organic cation transporter 1	*SLC22A4*
OCTN2	Novel organic cation transporter 2	*SLC22A5*
OAT1	Organic anion transporter 1	*SLC22A6*
OAT2	Organic anion transporter 2	*SLC22A7*
OAT3	Organic anion transporter 3	*SLC22A8*
OAT4	Organic anion transporter 4	*SLC22A9*

[a] Standardized names classified by the Human Gene Nomenclature Committee.

TABLE 1
Major drug transporters expressed in intestine, kidney, liver, and brain of human or rat

Human		Rat		Human		Rat	
Name	Localization	Name	Localization	Name	Localization	Name	Localization
Intestine				**Liver**			
Peptide transporter				*Organic anion transporter*			
PEPT1	BBM	PepT1	BBM	NTCP	SM	Ntcp	SM
				OATP-C	SM	Oatp1	SM
Organic anion transporter				OATP8	SM	Oatp2	SM
OATP-B	ND[a]	Oatp3	BBM	OATP-B	SM	Oatp4	SM
OATP-D	ND			OAT2	SM	Oat2	SM
OATP-E	ND					Oat3	SM
ASBT	BBM	Asbt	BBM			NaPi-1/Npt1	SM
Organic cation transporter				*Organic cation transporter*			
		Oct1	BLM	OCT1	ND	Oct1	SM
		Oct3	ND			Oct1A	ND
		Octn1	ND	OCT3			
Primary active transporter						Octn1	*ND*
MDR1	BBM	Mdr1	BBM	*Primary active transporter*			
MRP2	BBM	Mrp2	BBM	MRP1	SM		
MRP3	BLM	Mrp3	BLM	MRP3	SM	Mrp3 (EHBR, TR$^-$)	SM
BCRP	BBM						
				MDR1	CM	Mdr1	CM
				MRP2	CM	Mrp2	CM
Kidney				BSEP/SPGP	CM	Bsep/Spgp	CM
Peptide transporter				BCRP	CM		
		PepT1	BBM				
PEPT2	ND	PepT2	BBM				
				Brain capillary endothelial cells			
Organic anion transporter				*Organic anion transporter*			
OAT1	BLM	Oat1	BLM	OATP-A	ND	Oat2	ALM, LM
OAT3	BLM	Oat3	BLM			Oat3	ND
OAT4	BBM			*Organic cation transporter*			
						Oct2	ND
		Oatp1	BBM	*Primary active transporter*			
		Oat-K1	BBM	MDR1	LM	Mdr1	LM
		Oat-K1	ND			Mrp1	ND
		NaPi-1/Npt1	BBM			Mrp5	ND
		Asbt	BBM				
Organic cation transporter							
		Oct1	BLM	**Choroid plexus**			
		Oct1A	ND	*Peptide transporter*			
OCT2	BLM	Oct2	BLM			PepT2	BBM
		Oct3	ND	*Organic anion transporter*			
						Oatp1	BBM
OCTN1	ND	Octn1	BBM			Oatp2	BLM
OCTN2	ND	Octn2	BBM			Oatp3	BBM
Primary active transporter				*Primary active transporter*			
						Oat3	BBM
MDR1	BBM	Mdr1	BBM			Mrp1	BLM
MRP2	BBM	Mrp2	BBM			Mdr1	BBM
MRP4	BBM	Mrp4	BBM				

SM, sinusoidal membrane; CM, canalicular membrane; BLM, basolateral membrane; BBM, brush border membrane; LM, luminal membrane, ALM, abluminal membrane.
[a] ND, not determined.

(Lautier et al., 1996; Borst et al., 1999; Hooiveld et al., 2001; Lee et al., 2001a; Schinkel and Jonker, 2003). Most of the former transporters have a similar structure in that they have 12 putative membrane-spanning domains and their molecular mass is approximately 50 to 100 kDa. In contrast, the mean molecular weight of the latter transporters, involved in the cellular extrusion of xenobiotics, is comparatively high (150–200 kDa) and they all have two ATP-binding domains, except for BCRP. Furthermore, each gene family of transporters is composed of a multiplicity of members. Owing to the increase in the number of identified transporter genes, the Human Gene Nomenclature Committee has classified transporters using standardized names, such as the solute carrier superfamily (SLC) and ATP-binding cassette (ABC) transporters (http://www/gene.ucl.ac.ul/nomenclature/genefamily.shtml). These standardized names, accompanied by the conventional names, are shown in Table 2. The tissue distribution and elimination route of some drugs is determined by the degree of expression of each transporter subtype in each tissue and its corresponding substrate affinity and transport maximum. Thus, regulating the function of transporters should allow the highly efficient development of drugs with ideal pharmacokinetic profiles. As drug discovery involving the use of transport mechanisms increases, the need for an effective in vitro screening system for transporters will also increase. Accordingly, methods

TABLE 3
The putative molecular functions of 26,383 human genes (Venter et al., 2001)

	Number	%
Enzyme		
Hydrolase	1,227	4.0
Isomerase	163	0.5
Ligase	56	0.2
Lyase	117	0.4
Oxidoreductase	656	2.1
Synthase and synthetase	313	1.0
Transferase	610	2.0
Signal transduction		
Select regulatory molecule	988	3.2
Kinase	868	2.8
Receptor	1,543	5.0
Signaling molecule	376	1.2
Nucleic acid binding		
Nucleic acid enzyme	2,308	7.5
Transcription factor	1,850	6.0
None		
Transfer/carrier protein	203	0.7
Viral protein	100	0.3
Miscellaneous	1,318	4.3
Cell adhesion	577	1.9
Chaperone	159	0.5
Cytoskeletal structural protein	876	2.8
Extracellular matrix	437	1.4
Immunoglobulin	264	0.9
Ion channel	406	1.3
Motor	376	1.2
Structural protein of muscle	296	1.0
Protooncogene	902	2.9
Select calcium binding protein	34	0.1
Intracellular transporter	350	1.1
Transporter	533	1.7
Molecular function unknown	12,809	41.7

The functional predictions are based on similarity to sequences of known function.

PEPT1, expressed in tumors (Nakanishi et al., 1997, 2000). Some human cancer cell lines naturally express oligopeptide transport activity. The delivery of the peptide-mimetic anticancer drug, bestatin, a substrate of PEPT1, has been investigated. After i.v. administration of bestatin into nude mice-inoculated tumor cells, the bestatin concentration in PEPT1-transfected tumor was significantly greater than that in vector-transfected tumor (Nakanishi et al., 2000). Furthermore, repeated oral administration of bestatin specifically suppressed the growth of PEPT1-transfected tumors. It has been suggested that bestatin distributes to tumor tissues in a specific manner.

NTCP is the Na^+-bile acid cotransporting protein that mediates the hepatic uptake of bile acids (Hagenbuch et al., 1991). Since NTCP is exclusively expressed on the sinusoidal membrane of the liver (Meier, 1995), this transporter may be used as a target for drug delivery to that organ. Dominguez et al. have reported that coupling of drugs to the side chains of bile acids may be a useful strategy for specifically targeting liver tumor cells (Dominguez et al., 2001). A novel cisplatin-ursodeoxycholic derivative (Bamet-UD2) is efficiently transported by NTCP (Briz et al., 2002). The concentration of Bamet-UD2 in the liver was severalfold higher than that of cisplatin, while potentially toxic drug accumulation in other tissues, such as kidney, brain, and bone marrow, was significantly reduced (Dominguez et al., 2001). Thus, in mice, Bamet-UD2 exhibited strong antitumor activity without any side effects compared with cisplatin (Dominguez et al., 2001).

The targeting strategy should focus on the differential expression of transporters between the target organ and other organs, and it is essential to design molecules that are capable of being transported by a target organ-specific transporter. In particular, the use of blood-brain barrier (BBB)-specific influx transporters is expected to be an effective approach for the brain delivery of drugs acting on the central nervous system (CNS) because drug penetration into the brain is restricted under normal conditions.

B. Role of Brain Efflux Transporters

Brain capillary endothelial cells form the BBB and act as a self-defense mechanism, preventing xenobiotics from entering the brain. However, successful penetration of the blood-brain barrier is necessary if a drug is to reach the required concentration for a desired pharmacological effect. Efflux transport systems at such barriers provide protection for the CNS by removing drugs from the brain and transferring them to the systemic circulation. This is why the brain penetration of drugs is markedly restricted (Suzuki et al., 1997; Tsuji and Tamai, 1997; Fromm, 2000; Kusuhara and Sugiyama, 2001b; Lee et al., 2001a; Schinkel, 2001; Hagenbuch et al., 2002; Sun et al., 2003). Primary active transporters, such as P-gp encoded by MDR1 or MRP transporters, are responsible for the cellular extrusion of many kinds of drugs (Cole and Deeley, 1998; Borst et al., 1999; Kool et al., 1999; Kuwano et al., 1999). P-gp transports a wide variety of lipophilic, structurally diverse drugs, such as vinca alkaloids and anthracyclines. In general, the substrate specificities of efflux transporters are remarkably broad, and their affinities for substrates are much lower (of the order of micromolar to millimolar) than the affinities for pharmacological receptors (of the order of nanomolar to picomolar). Thus, these transporters are able to recognize a large number of xenobiotics with a wide variety of structures. In normal tissue, P-gp is expressed in the liver, kidney, small and large intestine, and brain capillary endothelial cells (Troutman et al., 2001) (Table 1). Thus, the brain penetration of drugs, which are substrates of this transporter, is extremely limited (Fromm, 2000; Tamai and Tsuji, 2000; Kusuhara and Sugiyama, 2001b; Schinkel, 2001). In mice that lack P-gp encoded by the mdr1a gene, the brain distribution of P-gp substrates is significantly increased compared with that in normal mice (Table 4). Clearly, these results demonstrate that P-gp plays a key role in the BBB. The transporter gene knockout mouse is a very important tool for investigating the role of transporters in drug disposition (Schinkel et al., 1994; Wijnholds et al., 1997, 2000; Jonker et al., 2001). Efflux transport should be taken